Journal of Hydrology 408 (2011) 257–275

Contents lists available at SciVerse ScienceDirect

Journal of Hydrology

journal homepage: www.elsevier.com/locate/jhydrol

Arid zone groundwater recharge and salinisation processes; an example from the Lake Eyre Basin, Australia

Sarah Tweed [a,b,*], Marc Leblanc [a,b], Ian Cartwright [b,c], Guillaume Favreau [d], Christian Leduc [e]

[a] School of Earth and Environmental Sciences, James Cook University, PO Box 6811, Cairns, QLD 4870, Australia
[b] National Centre for Groundwater Research and Training, Flinders University, Adelaide SA 5001, Australia
[c] School of Geosciences, Monash University, Melbourne, VIC 3800, Australia
[d] IRD, UMR HydroSciences, University of Montpellier cc MSE, 34095 Montpellier Cedex 5, France
[e] IRD, UMR G-Eau, BP 5095, 34196 Montpellier Cedex 5, France

ARTICLE INFO

Article history:
Received 9 December 2009
Received in revised form 17 April 2011
Accepted 6 August 2011
Available online 16 August 2011

This manuscript was handled by Laurent Charlet, Editor-in-Chief, with the assistance of Philippe Négrel, Associate Editor

Keywords:
Arid zone
Recharge
Salinity
Groundwater
MODIS data
Australia

SUMMARY

In arid central Australia, the ~1.14 M km^2 endorheic Lake Eyre Basin (LEB) experiences sporadic floods, and contains saline shallow groundwater. In this basin, where on-ground physical and chemical data are very sparse, new observations of major ion chemistry, stable isotopes (δ^2H, $\delta^{18}O$, $\delta^{13}C$), radiogenic isotopes (^3H, ^{14}C), and remote sensing (MODIS) data were used to investigate groundwater recharge and salinisation processes in 2006–2007. In January 2007 there was a large and intense local rainfall event, followed by flooding to the normally dry Lake Eyre resulting from heavy rainfall in the northern LEB that took ~2 months to arrive at Lake Eyre. Groundwater chemistry from this study show no evidence of recharge from the floodwaters or the local rainfall; however this does not preclude the process. Low transit times and low infiltrating volumes may mean that the recharge event has not yet been detected. Over the longer term, the stable isotope chemistry indicates that groundwater is predominantly diffusely recharged during heavy local rainfall events (>100–150 mm/month), and radiogenic isotopes reflect an older shallow groundwater efficiently mixing with recent (decadal) recharge. The high total dissolved solids (TDS) of regional shallow groundwater (up to 52.5 g/L) is intrinsically linked with these recharge processes; where infiltrating diffuse rainfall is evaporated, and heavy rainfall events transport saline pore water (saline due to evaporation in the unsaturated zone) to the groundwater system. The high TDS of shallow groundwater beneath the dry Lake Eyre bed (up to 322 g/L) is also controlled by evaporation. However, although evaporite minerals are prolific in the lake area, the non-conservative behaviour of Br in pore water limits analysis of the role of halite mineral dissolution and precipitation reactions controlling groundwater salinity. Evaporation-driven salinisation of shallow groundwater in arid central Australia is distinct from the transpiration-driven salinisation of groundwater in the Australian Murray Basin (located in a semi-arid climate), and results in relatively high groundwater salinity values compared with many other large arid zone endorheic basins across the world.

1. Introduction

Arid zones are exposed to extreme deficits of water due to low rainfall and relatively high evapotranspiration rates. In these regions, the effective evaporation or transpiration of infiltrating rainfall can result in low groundwater recharge rates and saline soil water and groundwater. In a large endorheic basin located in the arid zone of central Australia, the links between groundwater recharge and salinisation processes are explored.

Variations and changes in salinity, in time and/or in space, may reveal some of the processes affecting recharge and transfer of groundwater. This understanding is important in desert environments because groundwater can play an essential role in replenishing the groundwater system (Simmers, 2003), supporting ecosystems (e.g. Lubczynski, 2009) and, where quality permits, can provide an invaluable resource for local agricultural and domestic purposes (e.g. Tang et al., 2004; Al-Katheeri, 2008). A major water resource issue in most arid and semi-arid environments is groundwater salinisation. Processes resulting in high levels of primary groundwater salinisation can include evaporation (e.g. Ma et al., 2005), transpiration (e.g. Herczeg et al., 2001; Cartwright et al., 2008), seawater intrusion in coastal environments (e.g. Weyhenmeyer et al., 2002), and recycling of evaporites (e.g. Druhan et al., 2008).

* Corresponding author at: School of Earth and Environmental Sciences, James Cook University, PO Box 6811, Cairns, QLD 4870, Australia. Tel.: +61 7 4042 1468; fax: +61 7 4042 1284.

E-mail addresses: sarah.tweed@jcu.edu.au (S. Tweed), marc.leblanc@jcu.edu.au (M. Leblanc), ian.cartwright@monash.edu (I. Cartwright), Guillaume.Favreau@ird.fr (G. Favreau), Christian.Leduc@ird.fr (C. Leduc).

0022-1694/$ - see front matter © 2011 Elsevier B.V. All rights reserved.
doi:10.1016/j.jhydrol.2011.08.008

Often in semi-arid and arid environments, understanding recharge processes is inherent to understanding the salinisation processes. Recharging water can be fresh, therefore resulting in a 'freshening' of groundwater. For example, focused recharge via gullies or river floods can efficiently transport low salinity water to the groundwater system (e.g. Dahan et al., 2008; Favreau et al., 2009). In comparison, recharging water can be saline. Where slow diffuse recharge occurs, evaporation or transpiration process can result in saline residual water recharging the groundwater system (e.g. Cartwright et al., 2007a). Additionally, in arid and semi-arid environments recharging water may mobilise evaporites and saline pore water accumulated in the soil or in the deeper unsaturated zone (e.g. Rabemanana et al., 2005; Massuel et al., 2006; Scanlon et al., 2009).

Challenges in identifying these hydrologic processes within (semi-) arid environments generally include insufficient physical monitoring data across large areas, difficult field conditions in remote regions, and processes such as recharge being spatially and temporally highly variable (e.g. Simmers, 1997) because of the intermittent nature of recharge events (e.g. Allison et al., 1994). Increasingly, hydrochemical techniques are incorporated into studies to help investigate recharge processes and rates, and these include using conservative ions such as chloride (e.g. Edmunds and Gaye, 1994; Subyani and Şen, 2006; Gates et al., 2008), and environmental isotopes (e.g. Favreau et al., 2002; Harrington et al., 2002; Zongyu et al., 2005; Cartwright et al., 2006; Hutchison and Hibbs, 2008). In addition to chemical tracers, remote sensing techniques can also be incorporated to determine surficial influences on hydrogeological processes (e.g. Hoffmann, 2005; Leblanc et al., 2007, 2011). The ability to observe catchment-scale processes systematically, the access to temporal archives and the capacity to upscale site-specific measurements make remote sensing techniques increasingly attractive for constraining groundwater recharge processes. Links between surficial features and groundwater recharge processes have been established using aerial photographs (Leblanc et al., 2008), soil moisture data (e.g. Jackson, 2002), temperature patterns (e.g. Bobba et al., 1992; Leblanc et al., 2003a), and more commonly relating geological and geomorphic features to permeability (e.g. Salama et al., 1994; Leblanc et al., 2003b; Tweed et al., 2007).

In this study, groundwater recharge and salinisation processes are investigated in a large, endorheic arid basin by incorporating hydrochemical data with remote sensing data. Cl/Br ratios, $\delta^{18}O$ and $\delta^{2}H$ values, ^{3}H contents and ^{14}C activities are used to determine long-term groundwater salinity and recharge processes. The combination of these hydrochemical datasets with inundation mapping (MODIS) are used to investigate whether significant groundwater recharge has occurred during a river flood and heavy rainfall event in 2007. We investigate (1) whether groundwater is recharged predominantly by diffuse rainfall or by infiltration of river floodwater, and (2) the factors controlling groundwater salinity in the shallow aquifers of the central Australian desert.

1.1. Lake Eyre Basin

The study area is located in the Lake Eyre Basin, central Australia (LEB; Fig. 1). The LEB is a ~1.14 M km^2 internal drainage basin, with a population density of approximately 1 person/km^2. The endorheic Lake Eyre, located in the south of the basin, has a maximum surface area of 9500 km^2 and is the point of lowest elevation in Australia (~−15 mAHD). The LEB is located within the semi-arid and arid zones of Australia, and the study area is located in the arid zone (Fig. 1). The mean annual rainfall ranges between 140 in the Lake Eyre region and 260 mm in the NE at Boulia (106 years of data

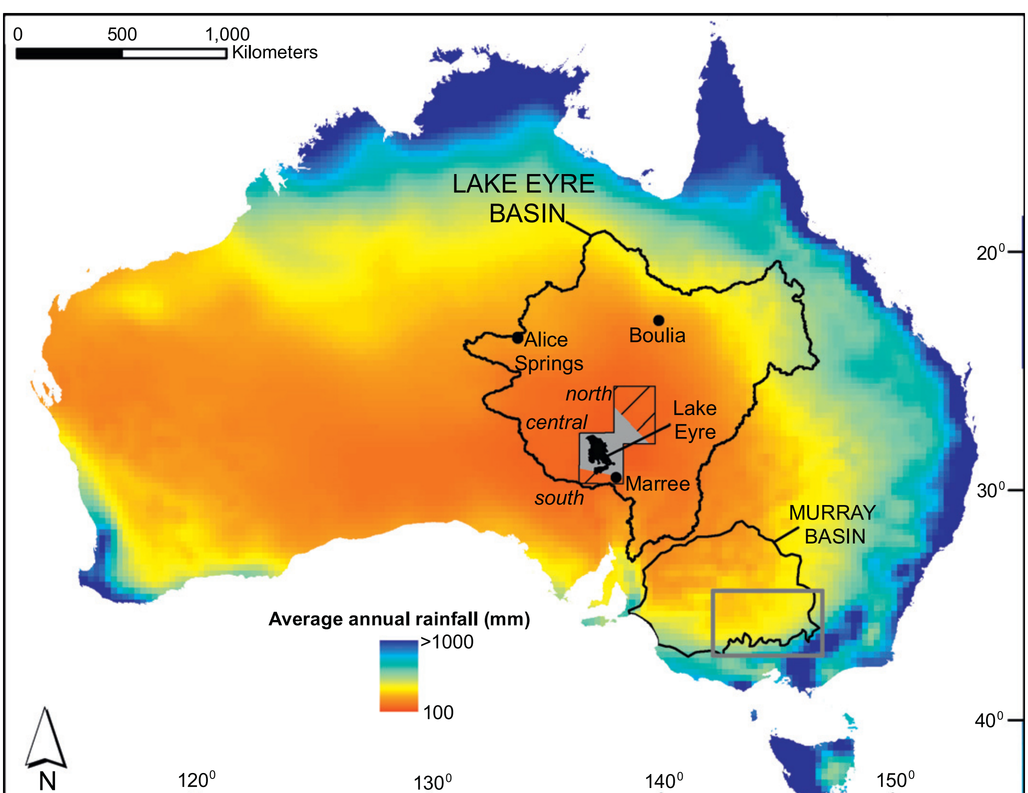

Fig. 1. Location of the Lake Eyre Basin (LEB) and the Murray Basin (MB) in central and SE Australia. The north, central and southern regions of the study area within the LEB are shown, and the rectangle within the MB is where data cited in this study were collected. Average annual rainfall levels are also shown (data from the Australian Bureau of Meteorology, 1900–2006).

from Bureau of Meteorology, 2006); the mean annual evaporation exceeds rainfall over the whole basin (2800–4000 mm based on 1975–2005 records from Bureau of Meteorology, 2006). In the northern region of the basin, intermittent large and intense rainfall events occur, which are often associated with La Niña episodes (e.g. Kotwicki and Allan, 1998; Puckridge et al., 2000). These irregular large rainfall events can result in short and large-scale flooding (e.g. Costelloe et al., 2006), that usually result in the inundation of Lake Eyre predominantly fed by the Diamantina River, and to a lesser extent by the Cooper Creek and Georgina River (Fig. 2; McMahon et al., 2008). Lake Eyre has recently received water from these rivers (early 2009 and early 2007), and previously has contained significant amounts of water during 1949/1950, 1974/1978, 1984/1985, 1985/1986, 1997 and 2000 (Williams, 2002). Such floods are essential in supporting abundant and diverse wildlife (e.g. Kingsford and Porter, 1993; Roshier et al., 2001; Sheil et al., 2006). Recent studies have reported high transmission losses during flood events along the Diamantina River, (e.g. McMahon et al., 2008). A study by Costelloe et al. (2007) also found that following the flood event in 2000, the water level fluctuations in a channel off the Diamantina River was linked with fluctuations of nearby shallow groundwater.

The landscape to the north of Lake Eyre is predominantly clay plains and floodplains (comprising grey and brown deep cracking clays), and dunefields of siliceous sands (Wright et al., 1990). To the south there are the stoney tablelands that consist of scarp ridges, plains with low sandy rises, sandy plains and stoney downs (Wright et al., 1990). Although the LEB is largely arid, the land has supported cattle grazing since European settlement in the 1800s (Hesse et al., 2004). The vegetation is dominated by arid grasses, Chenopodiaceous and Acacia shrublands (e.g. Martin, 2006), and in the riparian zones eucalyptus trees are common (dominated by Eucalyptus coolabah; Costelloe et al., 2008). Impacts of agriculture on the land surface are observed in changes in vegetation types, erosion and changes in soil drainage properties (e.g. Wright et al., 1990; Johnson et al., 2005). As discussed further below, unlike processes in the Murray Basin, the impact of agricultural practices on the water budget in the LEB remains largely unknown.

1.1.1. Local hydrogeology

The study area consists of two groundwater systems, the unconfined Tertiary–Quaternary aquifer system, which unconformably overlies the confined aquifers of the Eromanga Basin (Jurassic–Cretaceous). The Eromanga Basin aquifers form part of the Great Artesian Basin (GAB). The confining units that hydraulically separate the Eromanga Basin aquifers from the overlying Tertiary–Quaternary aquifers are the shales and mudstones of the Rolling Downs Group (Radke et al., 2000). This group of sediments ranges in thickness from ~400 to 1000 m in the study area (Radke et al., 2000), and is from 0 to >100 m below the surface (Moussavi-Harami and Alexander, 1998).

The unconfined Tertiary–Quaternary aquifer system (herein referred to as the Cenozoic aquifer) is comprised of fluvial sands, gravels, swamp deposits, and silcrete (Eyre Formation), which are overlain by continental dolomite, clays and sand (Etadunna Formation) (Magee et al., 1995). The deposition of these sediments was followed by the floodplain and lake deposits of the Tirari Formation (sand, silts, and clays), and then the aeolian deposition of the Simpson sands (Kreig et al., 1990). Within the study region, the total thickness of the unconfined aquifers ranges from approximately ~1 km in the northeast and decreases south toward the basin margin (Fig. 3). Evaporites are abundant in the Quaternary deposits, and are dominated by halite and gypsum (Magee et al., 1995). Halite is present as a salt crust at the surface of Lake Eyre (maximum recorded thickness of 46 cm in 1972), and sub-surface halite has also been found in cores from the lake bed (Magee et al., 1995).

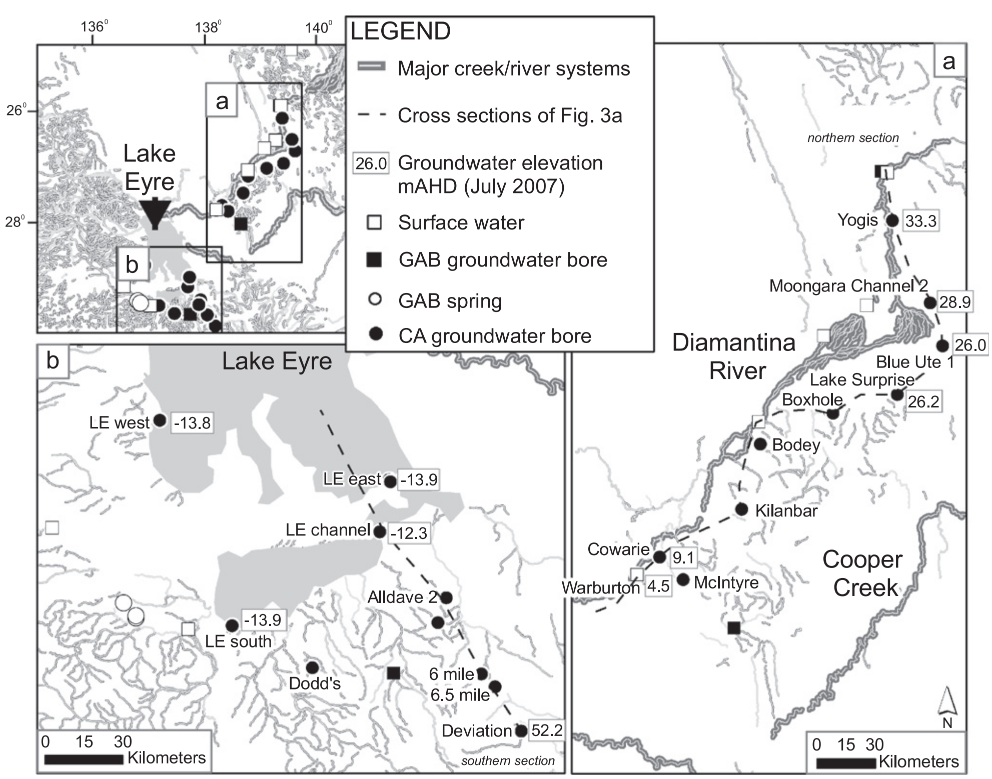

Fig. 2. Locations of groundwater sampled from bores and springs of the Great Artesian Basin (GAB), groundwater sampled from bores in Cenozoic aquifer (CA), and surface water (lake and creeks). The samples were collected from (a) sites close to the Diamantina River and floodplain to the north of Lake Eyre, and (b) from within and to the south of Lake Eyre. Also shown are the values of the groundwater hydraulic head measurements (from June 2007) that were corrected for density.

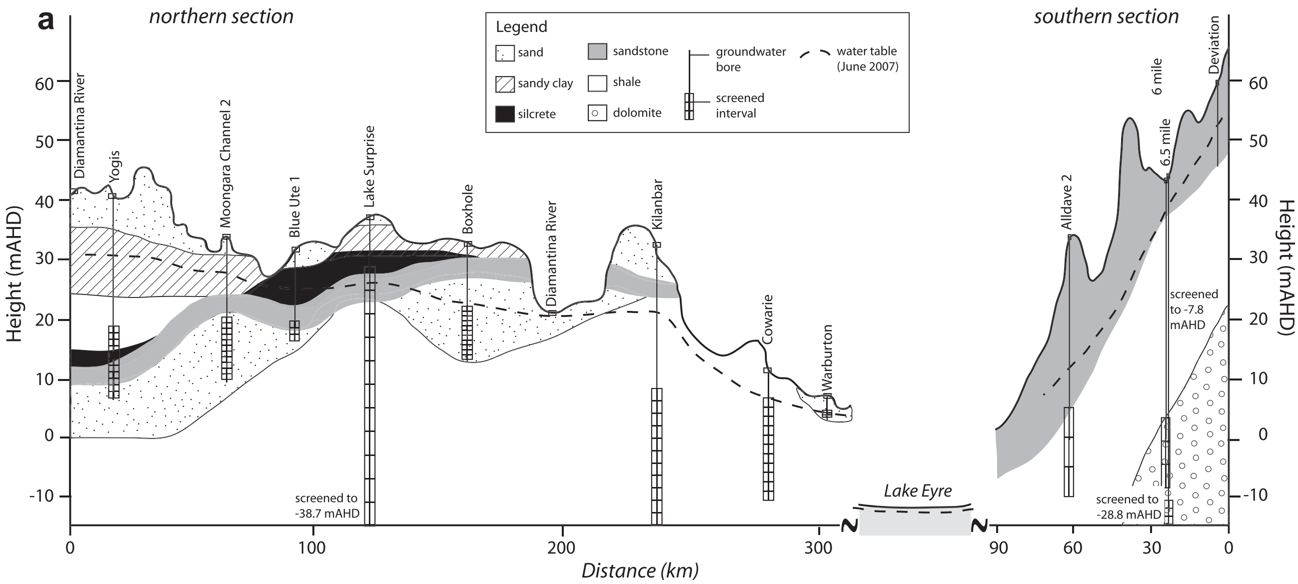

b

						(Bodey)	(McIntyre)			*west*	*east*	*south*				
TDS (g/L)	10.6	45.2-52.5	8.48	6.76-8.12	7.42	14.2	21.1	20-20.2	3.96	*26.6-62*	*81.8-92.3*	*10.3-14.1*	22.7	7.17	28.5	17
$\delta^2H_{activity\text{-}e}$	21	31-33	28	17-19	27	28	29	16-19	30	*19-22*	*31-34*	*48-52*	24	16	28	16
$A^{14}C$ (pmC)		89.3					79.2	65.1		*102.7*	*104.2*		70.1			
^3H (TU)		2.9					1.3	0.9		*3.5*	*2.8*		2.3			

Fig. 3. (a) Schematic cross-section of study region, from north to south of Lake Eyre (location of section shown in Fig. 2). The geology (taken from drillers bore logs), groundwater elevation, screen details for some of the groundwater bores sampled, and topography (SRTM) are presented. (b) Groundwater chemistry results for bores located along the northern and southern sections, and from the Lake Eyre shoreline (bores in parenthesis were not used for cross-section); $\delta^2H_{activity\text{-}e}$ is the enrichment of the $\delta^2H_{activity}$ relative to the average rainfall estimate of −57‰, and all sample round results are presented.

Gypsum crystals up to 3 cm are present but are more commonly between 0.01 and 1 cm (Magee et al., 1995).

Within the Cenozoic aquifer, general groundwater flow directions are towards Lake Eyre (Fig. 2). Our observations indicate the water table depths (corrected for density) in the Lake Eyre bed range from 0 to 1.10 m (Table 1). The artesian groundwater of the GAB discharges via springs in the southern and southwestern areas of the LEB. The extent of groundwater mixing between Cenozoic aquifer and the underlying confined GAB is unknown, however it is suspected that there is diffuse upward leakage of the artesian groundwater into the Cenozoic aquifer. Proximal to Lake Eyre, the confining shale formation between the GAB and the Cenozoic aquifer locally crops out or is close to the surface (Fig. 3a), and can be significantly altered, which potentially results in diffuse discharge of GAB groundwater. However, as discussed below, results from this study show that major ion and stable isotope chemistry of groundwater from the GAB and Cenozoic aquifer remain geochemically distinct.

The shallow groundwater of the Cenozoic aquifer is saline, whereas the underlying confined GAB groundwater system is relatively fresh. The fresher GAB groundwater (average TDS of 1.9 g/L from 663 samples; Radke et al., 2000) provides water for agriculture, domestic and mining practices in central Australia (e.g. Mudd, 2000). The saline groundwater in the Cenozoic aquifer (TDS: 5–322 g/L; average of 73.2 g/L from 28 values in this study) has limited uses. As a result, compared with geochemical studies on the GAB (e.g. Herczeg et al., 1991; Love et al., 2000; Radke et al., 2000; Pirlo, 2004), relatively little is known about the shallow groundwater system. Recent studies by Costelloe et al. (2009) and Cendón et al. (2010) in the east of the Lake Eyre Basin (Cooper Creek) found that young saline groundwater in the shallow aquifer is intermittently recharged via ephemeral lakes or waterholes during inundation events. Otherwise, to our knowledge, there is a lack of information about recharge processes occurring and the controls on regional groundwater salinity for the Cenozoic aquifer.

2. Data and methods

2.1. Climate data

Climate data are from the Australian Bureau of Meteorology (http://www.bom.gov.au). Gridded monthly rainfall data (0.05° resolution, and a station data accuracy of 0.01°) for the period January 2006 to July 2007 were used to calculate spatial averages over the entire study area, and over 3 defined zones within this area; north, central and south (Fig. 1). To indicate rainfall intensity for the month of January 2007, mosaic archives from the National Radar network, and daily gridded rainfall data were also used. The radar mosaics clearly show rain and storm activity surrounding the study area between 17th and 19th January 2007. Daily gridded rainfall data for the study area also shows that most rainfall activity occurred over 4 days in January (18th–21st), therefore indicating a high intensity associated with the relatively large rainfall levels for the month of January 2007.

2.2. Mapping inundated areas

The Moderate Resolution Imaging Spectroradiometer (MODIS) provides new remote sensing opportunities for global monitoring of land and water resources (Justice et al., 2002). To monitor the extent of inundated area in the LEB we acquired a time series of MODIS/TERRA surface reflectance product, MOD09A1 Version 005, from January 2007 to July 2007 (data distributed by the Land Processes Distributed Active Archive Center, http://lpdaac.usgs.gov, US Geological Survey, Earth Resources Observation and

Table 1
Sample locations, groundwater elevations and major ion concentrations for groundwater (GAB and Cenozoic aquifer) and surface water (lakes and creeks). Groundwater and surface water sampled more than once are highlighted in grey.

Sample name	Sample type[a]	Date	Lat	Long	Bore screen interval (m)	Depth to water table (m)[b]	GW (mAHD)[b]	Temp (°C)	pH	HCO_3 (mg/L)	CO_2 (mg/L)	Cl (mg/L)	Br (mg/L)	NO_3 (mg/L)	SO_4 (mg/L)	Na (mg/L)	K (mg/L)	Ca (mg/L)	Mg (mg/L)	Si (mg/L)	TDS (mg/L)	Cl/Br ratio	Halite SI[c]	Gypsum SI[c]
Birdsville artesian bore	GAB	July-2006	−25.8978	139.3483	–	–	–	55.4	8.44	421		34	0.4	0.3	nd	200	7	2	nd	35.0	783	174		
Brolga bore	GAB	July-2006	−29.6451	137.7531	–	–	–	23.8	8.10	1089		1210	4.3	nd	66	777	16	8	6	8.6	3300	630		
Maree bore	GAB	July-2006	−29.6472	138.0588	92–116, 152–200	–	–	18.9	7.59	931		1100	3.7	nd	60	1070	15	20	13	7.4	3350	665		
Blanche cup spring	GAB	July-2006	−29.4529	136.8587	–	–	–	14.9	7.31	828	154	2510	10.1	5.9	326	1490	50	72	40	4.2	5500	559		
Coward springs	GAB	July-2006	−29.4006	136.8147	–	–	–	30.0	6.88	987	162	1340	7.5	6.0	168	1210	43	29	27	5.5	3990	401		
Bubbler spring	GAB	July-2006	−29.4464	136.8580	–	–	–	29.2	6.95	977	180	1580	10.4	6.1	151	1180	42	30	26	5.1	4190	343		
Lake Eyre channel bed	CA	June-2007	−29.1532	137.7064	0–0.8	0.29	−12.29	21.9	6.75	66	540	173,000		52.4	11,600	80,900	462	580	1890	nd	269,000	12,200	−0.16	0.27
Lake Eyre east bed	CA	July-2006	−28.9716	137.7384	0–2	1.10	−13.10	18.5	6.88	73	274	198,000	42.6	43.1	3210	101,000	361	743	1620	0.5	305,000	10,500	0.15	−0.02
Lake Eyre east shoreline	CA	July-2006	−28.9790	137.7428	1.95–3.45	1.79	−13.79	18.4	7.16	134	114	45,600	104.6	61.2	5250	27,900	185	1680	727	13.5	81,800	983	−1.68	0.13
Lake Eyre east shoreline	CA	November-2006	−28.9790	137.7428	2–2.56	1.95	−13.95	25.9	6.77	–	–	–	–	–	–	–	–	–	–	–	–	–	–	–
Lake Eyre east shoreline	CA	June-2007	−28.9790	137.7428	2–2.56	1.92	−13.92	18.0	–	224	136	54,800	–	45.1	6780	27,800	163	1590	757	nd	92,300	6300	−1.59	0.21
Lake Eyre south bed	CA	June-2007	−29.4799	137.1931	0–1	0.01	−12.01	12.9	6.50	234	320	198,000	–	11.0	9220	98,500	546	683	1050	nd	309,000	13,000	0.14	0.4
Lake Eyre south shoreline	CA	July-2006	−29.4859	137.1898	2–2.56	1.70	−13.70	25.0	7.21	124	120	83,600	333	58.4	13,200	41,700	241	1140	885	1.8	141,000	567	−1.14	0.35
Lake Eyre south shoreline	CA	June-2007	−29.4859	137.1898	2–2.56	1.93	−13.93	24.8	6.91	195	60	62,500	–	30.1	6720	31,400	245	1050	996	nd	103,000	11,400	−1.46	0.12
Lake Eyre west bed	CA	November-2006	−28.7690	136.9421	0–0.4	0.00	−12.00	24.8	6.50	124	120	201,000	42.4	5.7	7890	105,500	1590	538	4920	1.4	322,000	10,700	0.25	0.1
Lake Eyre west shoreline	CA	July-2006	−28.7645	136.9416	1.33–2.33	1.80	−13.80	20.7	7.20	158	106	35,600	94.9	39.0	4270	19,500	105	1680	382	12.2	62,000	846	−1.97	0.1
Lake Eyre west shoreline	CA	November-2006	−28.7645	136.9416	1.33–2.33	1.82	−13.82	25.5	6.84	–	–	–	–	–	–	–	–	–	–	–	–	–	–	–
Lake Eyre west shoreline	CA	June-2007	−28.7645	136.9416	1.33–2.33	1.78	−13.78	21.2	6.99	212	216	15,600		10.5	917	7600	45	1500	434	7.3	26,600	11,000	−2.74	−0.43
6 mile bore	CA	July-2006	−29.6881	138.1043	54–72	5.18	37.96	21.7	7.73	760		3360	4.5	28.7	nd	2700	67	43	49	7.2	7170	1670	−3.77	−7.39
6.5 mile bore	CA	November-2006	−29.6920	138.1064	40–52	3.15	40.93	29.6	6.76	597	392	12,700	62.1	28.2	4730	8610	96	796	509	13.5	28,500	461	−2.78	−0.04
Alldave2	CA	November-2006	−29.3823	137.9370	29–44	21.64	12.61	27.9	6.53	171	240	9940	38.5	12.3	4400	6380	93	1120	257	17.1	22,700	582	−3.01	0.14
Blue ute 1	CA	June-2007	−26.7108	139.6323	12–15.4	6.30	26.00	19.2	7.44	83	150	3180	–	103	2190	1660	34	849	211	13.2	8480	2800	−4.03	−0.02
Bodey bore	CA	July-2006	−27.1649	138.7866	14–26, 38–56	9.77	20.02	26.5	7.08	290	142	6230	35.3	nd	2620	4150	61	456	160	35.2	14,200	398	−3.37	−0.29
Boxe hole bore	CA	July-2006	−27.0206	139.1240	10.5–19.5	10.91	21.72	25.2	7.12	68	46	2960	10.3	33.9	1650	1710	60	739	103	34.5	7420	649	−4.04	−0.13
Cowarie	CA	November-2006	−27.6902	138.3179	5–23	4.73	9.13	35.5	6.67	161	98	9950	22.1	6.9	3000	5150	80	1410	225	38.9	20,200	1010	−3.1	0.12
Cowarie	CA	June-2007	−27.6902	138.3179	5–23	4.77	9.09			132	126	9970	–	7.9	3140	5120	18	1240	204	15.1	20,000	6980	−3	0.09
Deviation bore	CA	June-2007	−29.8459	138.1978	–	7.03	52.21	19.0	6.64	248	566	7280	–	19.6	2070	3800	24	2550	403	nd	17,000	11,900	−3.36	0.16
Dodd's bore	CA	July-2006	−29.6255	137.4715	–			19.9	6.91	322	142	7260	15.4	nd	2410	5740	98	485	598	6.7	17,100	1070	−3.18	−0.41
Kilanbar bore	CA	July-2006	−27.4678	138.6989	24–48, 66–78	11.86	23.12	25.6	7.39	140	72					3730	58	827	117	24.1				
McIntyre1	CA	November-2006	−27.7968	138.4268	17–29	19.20	11.52	34.8	7.07	127	80	3000	12.7	8.0	2260	1630	74	970	104	29.4	8300	534	−4.06	0.07
Lake surprise bore	CA	June-2007	−26.9373	139.4229	8–74	10.48	26.16	16.3	7.02	29	124	3280		47.4	1830	1690	29	935	133	13.9	8120	4960	−4.01	−0.03
Lake surprise bore	CA	July-2006	−26.9373	139.4229	8–74	10.85	25.79	25.6	7.27	78	48	2450	6.5	37.0	1330	1520	59	1080	95	31.5	6760	852	−4.17	−0.08
Warburton Ground	CA	June-2007	−27.7739	138.2125	5–6	3.28	4.46	17.3	7.17	628	278	23,100		26.4	2120	10,700	90	1790	842	21.4	39,600	4870	−2.43	−0.12
Moongara channel 2	CA	July-2006	−26.5102	139.5757	13.5–24	5.61	29.03	26.8	6.69	132	168	29,500	88.2	195	3160	15,500	82	2390	1210	12.3	52,500	754	−2.16	0.09
Moongara channel 2	CA	November-2006	−26.5103	139.5757	13.5–24			31.6	6.83	–	–	–	–	–	–	–	–	–	–	–	–	–	–	–
Moongara channel 2	CA	June-2007	−26.5103	139.5757	13.5–24	5.71	28.93	14.4	6.30	139	184	26,200		202	2800	12,300	43	2150	1040	5.6	45,200	2330	−2.31	0.03
Yogis bore	CA	June-2007	−26.1258	139.4004	21–33	9.13	33.31	21.1	6.94	339	292	4140	–	6.9	3340	2040	14	264	118	14.8	10,600	1780	−3.84	−0.34
Diamantina Birdsville	SW	July-2006	−25.9035	139.3751	–	–	–	12.8	8.18	41		55	0.2	0.2	6	34	4	7	2	14.2	266	686		
Diamantina Birdsville	SW	June-2007	−25.9035	139.3751	–	–	–	12.0	7.73	76		41	–	0.4	4	22	4	7	2	16.2	227	555		
Diamantina channel	SW	July-2006	−26.6654	139.0809	–	–	–	9.2	7.70	166		84	0.3	0.3	5	56	8	18	5	20.7	396	592		
Diamantina Kalamurina	SW	June-2007	−27.7732	138.2128	–	–	–	15.2	9.12	275		143	–	0.6	71	150	11	141	70	2.5	977	729		
Diamantina New Alton Downs	SW	July-2006	−26.5221	139.2799	–	–	–	10.2	7.83	56		54	0.4	1.3	12	17	4	6	2	15.9	198	321		
Diamantina simpson	SW	June-2007	−27.0629	138.7769	–	–	–	12.2	8.12	163		93	–	0.9	8	72	6	14	4	8.4	508	715		
Lake Kolivoo	SW	July-2006	−24.8997	139.5597	–	–	–			72		98	1.0	0.9	22	13	5	13	4	8.2	264	211		
Margaret creek	SW	June-2007	−29.4912	137.0408	–	–	–	15.6	8.66	90		2560	–	0.2	122	1340	20	159	44	0.9	4400	730		
Warriners creek	SW	June-2007	−29.1386	136.5673	–	–	–	15.8	7.86	146		8150	–	1.6	2420	4750	118	717	224	1.2	16,600	712		
Salt crust of Lake Eyre (halite)		November-2006	−28.9716	137.7384								188	0.04		45	116	0.9	7	nd			10,600		
Unsaturated zone salt (gypsum)		November-2006	−28.7690	136.9421								2.1	nd		721	3	0.7	217	0.1					

[a] CA is groundwater sampled from the Cenozoic aquifers.
[b] Corrected for density.
[c] SI is the saturation index calculated using Phreeqc (Parkhurst and Appelo, 1999).

Science). MOD09A1 scenes offer weekly coverage of the Lake Eyre Basin in seven bands ranging from the visible to the middle infrared part of the electromagnetic spectrum with a spatial resolution of ~500 m. MOD09A1 are composite images where each pixel contains the best possible observation during an 8-day period as selected on the basis of high observation coverage, low view angle, the absence of clouds or cloud shadow, and aerosol loading. All non-cloudy pixels of the surface reflectance product (MOD09A1) are defined as the reflectance that would be measured at the land surface if there were no atmosphere. Corrections were applied for the effect of gaseous absorption, molecules and aerosol scattering, coupling between atmospheric and surface bi-directional reflectance function (BRDF) and adjacency effect (Vermote et al., 1997; Vermote and Vermeulen, 1999).

MODIS band 5 was used to map the extent of shallow open water, and MODIS bands 1 and 2 were used to map the extent of water under aquatic vegetation. Shallow depths and high suspended sediment concentration, such as those observed along the Diamantina flood plain, increase considerably the amount of solar energy reflected by a water body (Engman and Gurney, 1991; Bukata, 2005). Li et al. (2003) showed that the strong water absorption at wavelength >1 μm in MODIS bands (bands 5, 6 and 7) does not allow illumination of the sediments in the water or at the shallow bottom of a water column. A simple combination of threshold technique was performed on MODIS band 5 to delineate all open waters including shallow, sediment laden open water bodies.

Water is also present under aquatic vegetation in the vast flood plains of the region. Aquatic vegetation and hydrophilic plants can mask underlying water and should be included in the inventory of inundated areas (e.g. Leblanc et al., 2003b). NDVI has been shown to be a robust index for monitoring temporal changes of the vegetation photosynthetic activity (e.g. Lyon et al., 1998; Lunetta et al., 2006). Because of the extreme arid climate in the region, a high level of vegetation photosynthetic activity can only be sustained by the presence of surface water or groundwater discharge. In these conditions it is possible to use a vegetation index, such as NDVI $((b2 - b1)/(b2 + b1))$, to separate aquatic vegetation from sparse, desertic vegetation on dryland. A threshold technique was used to select high NDVI values and detect areas of water under aquatic vegetation and hydrophilic plants, present in floodwaters in the LEB (e.g. Sheldon et al., 2002).

An airborne survey was carried out over large lakes of the region in November 2006 to determine the different threshold values. Reflectance values <20% in MODIS band 5 and NDVI values greater than 0.4 show the same extent of open water and aquatic vegetation as the airborne survey and were therefore used as threshold values in this study.

2.3. Groundwater, pore water and surface water sampling

Groundwater, pore water and surface water was sampled in July 2006, November 2006, and June 2007. Most groundwater samples are from the Cenozoic aquifer (31 samples from 21 locations), six samples are from the GAB confined aquifers, and nine surface water samples were collected in July-2006 and June-2007 (Tables 1 and 2). The locations of the groundwater and surface water samples are presented in Fig. 2a and b. Shallow groundwater piezometers (<3.5 m) were installed during the first sample round (7 around Lake Eyre), and groundwater was also sampled from selected bores owned by the Department of Road Transport, South Australia (15 bores). Pore water samples were collected from three locations in the lake bed. These unsaturated zone samples were collected at 10 cm depth intervals (ranging from 1 to 2 m in total depth) and were centrifuged on return to the laboratory.

The surface elevation of the study area was mapped using data from shuttle radar topographic mission of February 2000 (SRTM at 1 m vertical resolution). These elevation values were used to calculate hydraulic heads that were corrected for density (h_{density}) using the following relationship (Collins, 1975):

$$h_{\mathrm{density}} = 6 \times 10^{-13} \times \mathrm{TDS}^2 + 7 \times 10^{-7}\mathrm{TDS} + 1 \quad (1)$$

Groundwater samples from boreholes <5 m deep were collected using a polyethylene bailer, and deeper wells were micropurged using a submersible pneumatic bladder pump. Electrical conductivity (EC) was monitored during sampling; once stabilised samples were collected and pH and temperature were measured immediately at surface. Alkalinity and dissolved CO_2 were also measured in the field by titrations. Detection limits for alkalinity and dissolved CO_2 were 1.64 and 0.23 mol/L respectively, with precision of ~±10%.

Samples for cation analyses were filtered (0.45 μm cellulose nitrate filter) and acidified to pH < 2 (ultrapure 16 N HNO_3) in the field, and the analyses were performed using a Varian Vista ICP-AES at the Geochemistry Laboratory, Geology Department, Australian National University, Canberra. Unacidified samples for anions were analysed using a Metrohm ion chromatograph at Monash University, Melbourne. Results of cations and anions for groundwater and surface water are presented in Table 1. Br concentrations of groundwater from the June 2007 sampling round were omitted from analysis due to anomalously low concentrations. Charge balance errors for the GAB groundwater are −21% to −7% (standard deviation = 10), −24% to 24% (standard deviation = 11) for Cenozoic aquifer groundwater, and −39% to 27% (standard deviation = 19) for surface waters. For three of the Cenozoic aquifer groundwater samples, one GAB sample and four river water samples, errors were above ±15%. These larger charge balance errors are only associated with water with lower TDS concentrations (<17,000 mg/L), which therefore precludes systematic dilution or standardisation as the cause of the larger errors. Na and Cl show a good correlation (r^2 of the linear trendline = 0.997), therefore random dilution is not the cause. The errors may be a precision error associated with the field titration of HCO_3.

Stable isotope ratios (δ^2H, $\delta^{18}O$, and $\delta^{13}C$) were analysed using the Finnigan MAT 252 mass spectrometer at Monash University, Melbourne. The precision is $\delta^{18}O$ = ±0.1‰ and δ^2H = ±1‰. $\delta^{18}O$ values were measured via equilibration with CO_2 at 25 °C for 24–48 h, and δ^2H were measured via reaction with Cr (850 °C). A NaCl-rich internal standard with an EC of ~224,000 υS/cm was used to monitor the performance of the equipment for the analysis of saline waters, and data were normalised following Coplen (1988). CO_2 from dissolved inorganic carbon (DIC) was liberated by acidification using H_3PO_4 in a He atmosphere and analysed by continuous flow. $\delta^{13}C$ values are expressed relative to V-PDB. Precision based on replicate analyses is $\delta^{13}C$ = ±0.1‰. The results of stable isotopes are presented in Table 2, and the measured raw data for $\delta^{18}O$ and δ^2H are expressed as activities and concentrations respectively. The following relationship was used to correct δ^2H to activities (Horita, 1989):

$$\Delta\delta^2\mathrm{H} = -2.4m\mathrm{NaCl} - 5.1m\mathrm{MgCl_2} - 6.1m\mathrm{CaCl_2} - 2.4m\mathrm{KCl} \quad (2)$$

where m is molar concentration. The concentrations of $\delta^{18}O$ are related to activities by (Horita, 1989):

$$\Delta\delta^{18}\mathrm{O} = 0.8\mathrm{mMgCl} + 0.5\mathrm{mCaCl_2} - 0.1\mathrm{mKCl} \quad (3)$$

Data are presented in Table 2, which shows that the difference in the raw relative to the corrected values is greatest for δ^2H compared with $\delta^{18}O$.

Table 2
Stable isotope results for groundwater sampled from the GAB and Cenozoic aquifer (CA), local rainfall, and surface water (SW). Radiogenic isotope data are also presented for the Cenozoic aquifer groundwater. Groundwater and surface water sampled more than once for stable isotopes are highlighted in grey.

Sample name	Sample type	Date	$\delta^{18}O_{actlvlty}$ [a]	$\delta^{18}H_{activity}$ [b]	$\delta^{18}O_{concentration}$ [b]	$\delta^{18}H_{concentration}$ [a]	$\delta^{13}C$	$^{14}C_{activity}$	$\pm^{14}C_{activity}$	^{3}H	^{3}H [c]
			‰ V-SMOW	‰ V-SMOW	‰ V-SMOW	‰ V-SMOW	‰ V-PDB	pmC	Uncertainty	TU	Uncertainty
Birdsville artesian bore	GAB	July-2006	−7.2	−46.0	−7.2	−46.1					
Brolga bore	GAB	July-2006	−7.3	−46.8	−7.3	−47.3					
Maree bore	GAB	July-2006	−7.2	−42.7	−7.2	−43.2					
Blanche cup spring	GAB	July-2006	−6.7	−41.7	−6.7	−42.7					
Coward springs	GAB	July-2006	−7.1	−43.1	−7.1	−43.7					
Bubbler spring	GAB	July-2006	−7.1	−44.1	−7.1	−44.8					
6 mile bore	CA	July-2006	−5.5	−39.4	−5.5	−40.8	−6.1				
6.5 mile bore	CA	November-2006	−2.9	−24.8	−2.9	−30.2					
Alldave2	CA	November-2006	−3.4	−29.5	−3.4	−33.8	−14.8	70.1	0.3	2.3	0.08
Blue ute 1	CA	June-2007	−2.3	−27.5	−2.3	−29.0					
Bodey bore	CA	July-2006	−3.0	−27.1	−3.0	−29.8	−6.9				
Boxe hole bore	CA	July-2006	−2.6	−28.7	−2.5	−30.0	−7.3				
Cowarie	CA	November-2006	−3.1	−27.2	−3.1	−31.5	−14.2	65.1	0.3	0.9	0.03
Cowarie	CA	June-2007	−3.7	−34.4	−3.7	−38.6					
Deviation bore	CA	June-2007	−5.1	−38.7	−5.1	−42.1					
Dodd's bore	CA	July-2006	−4.2	−33.8	−4.2	−36.9	−13.2				
Kilanbar bore	CA	July-2006	−3.4	−33.8	−3.4	−33.8	−3.8				
Lake Eyre east bed	CA	July-2006	3.9	73.8	3.9	−7.4	−8.4				
Lake Eyre east shoreline	CA	July-2006	−0.9	−7.5	−0.8	−26.7	−8.7				
Lake Eyre east shoreline	CA	November-2006	−3.3		−3.3	−33.4	−16.1	104.2	0.5	2.8	0.09
Lake Eyre east shoreline	CA	June-2007	0.0	−6.6	0.0	−29.3					
Lake Eyre south bed	CA	June-2007	4.0	76.3	4.0	−5.0					
Lake Eyre south shoreline	CA	July-2006	5.1	24.4	5.1	−10.1	−5.6				
Lake Eyre south shoreline	CA	June-2007	5.5	12.9	5.5	−12.9					
Lake Eyre channel bed	CA	June-2007	5.8	64.1	5.9	−6.7					
Lake Eyre west shoreline	CA	July-2006	−3.9	−25.4	−3.9	−40.3	−8.9				
Lake Eyre west shoreline	CA	November-2006	−3.2		−3.1	−31.2	−15.2	102.7	0.5	3.5	0.20
Lake Eyre west shoreline	CA	June-2007	−3.3	−29.7	−3.3	−36.3					
McIntyre1	CA	November-2006	−2.1	−27.5	−2.1	−28.9	−13.1	79.2	0.3	1.3	
Lake surprise bore	CA	July-2006	−4.4	−38.9	−4.3	−40.1	−6.8				
Lake surprise bore	CA	June-2007	−4.2	−37.3	−4.2	−38.8					
Warburton Ground	CA	June-2007	−1.2	−18.8	−1.1	−28.5					
Moongara channel 2	CA	July-2006	0.2	−16.4	0.3	−28.9	−8.2				
Moongara channel 2	CA	November-2006	−3.0		−3.0	−30.5	−12.3	89.3	0.4	2.9	0.11
Moongara channel 2	CA	June-2007	0.6	−14.6	0.6	−25.7					
Yogis bore	CA	June-2007	−2.7	−34.9	−2.7	−36.6					
Rain tues 31 Oct 06	RAIN	November-2006	−5.7	−32.0	−5.7	−32.0					
Diamantina at Kalamurina	SW	June-2007	5.1	10.9	5.2	11.0					
Diamantina at New Alton Downs	SW	July-2006	−8.2	−50.7	−8.2	−50.7					
Diamantina Birdsville	SW	July-2006	−5.6	−44.3	−5.6	−44.3					
Diamantina Birdsville	SW	June-2007	3.3	−4.1	3.3	−4.1					
Diamantina Channel	SW	July-2006	3.6	−12.9	3.6	−12.9					
Diamantina simpson	SW	June-2007	7.7	19.1	7.7	19.1					
Margaret Cr	SW	June-2007	2.1	3.3	2.1	3.2					
Warriners Cr	SW	June-2007	2.1	1.6	2.1	1.3					

[a] Measured.
[b] Corrected.
[c] Due to evaporation (analytical uncertainty is ±0.2).

Six groundwater samples were analysed for ^{14}C activities ($a^{14}C$) and ^{3}H contents (Table 2). Groundwater bores sampled for these radiogenic isotopes all have screen intervals <20 m and the water table ⩽7 m above screened intervals. Groundwater in the basin is potentially exposed to large recharge events during increased rainfall periods between December and March. Therefore groundwater was sampled prior to the high rainfall period (November 2006) to reflect average groundwater ages. Percent modern carbon contents were determined by Accelerator Mass Spectrometry (AMS) at the Australian Nuclear Science and Technology Organisation (ANSTO), Australia. CO_2 from dissolved inorganic carbon (DIC) was liberated by acidification using H_3PO_4 in a He atmosphere and $\delta^{13}C$ values were measured using continuous flow on a Finnigan MAT 252 mass spectrometer at Monash University. $\delta^{13}C$ values are expressed relative to PDB and the precision (1σ) is ±0.2. Tritium content was analysed by scintillation counting after electrolytic enrichment. The uncertainty associated with ^{3}H results is 0.2 TU, and errors associated with ^{14}C results range from 0.31 to 0.54 pmC (percent of modern carbon).

3. Results

3.1. Rainfall and inundation

For the time period investigated (July 2006–June 2007) a relatively intense local rainfall event was recorded in January 2007 (maximum 148.7 mm), with the greatest rainfall occurring in the northern region (Fig. 4). Daily radar images and gridded rainfall maps highlight the rainfall of January 2007 occurred over a period of ∼4 days. The inundation mapping presented in Fig. 5b, using MODIS during 9–17 January 2007, shows that this rainfall event resulted in (1) ponding in topographic depressions, which covered a total surface area of ∼2300 km^2 (Fig. 5a). The inundated areas comprise open water including shallow water bodies, and water under aquatic vegetation.

Between January and July 2007 there was also flooding of the Diamantina River. The floods were the result of high rainfall in the northern LEB, rather than local rainfall. Fig. 5b shows that during 25-January and 2-February there was (2) the drying up of the ponding in Lake Eyre that was due to local rainfall, and (3) the arrival of the flood from the headwaters in the northern LEB. During 25-February to 6-March the (4) propagation of floodwaters continued along the Diamantina floodplain, and (5) the floodwaters arrived in Lake Eyre (Fig. 5b). During 14–22 March there is (6) flooding of Lake Eyre, and the area inundated peaks at ∼3400 km^2 (Fig. 5a). Therefore the floodwaters took ∼2 months to reach Lake Eyre.

Fig. 6 presents the total areas inundated, during both the local rainfall and the propagation of the floodwaters, over the 7 month period. The inundation mapping shows that most groundwater bores sampled are located outside of the floodwater area (Fig. 6). The distance between the floodwater and groundwater bores is up to ∼20 km at Kilanbar bore. Only the Lake Eyre west piezometer is located within this inundated area.

3.2. Major ions

Major ion chemistry is presented in Table 1. For groundwater from the Cenozoic aquifer, the TDS content ranges from 4980 to 322,000 mg/L. For six groundwater bores with temporal data (July and/or November 2006 to June 2007), there is no systematic change in groundwater TDS contents during the study period (Table 1). Prior to the rainfall event in January-2007, groundwater TDS content ranges from 6760 to 141,000 mg/L, and for the same bores in Jun-2007 groundwater TDS contents ranges from 8120 to 103,000 mg/L; resulting in percentage changes ranging from −57% to 20%. For individual major ion concentrations results show that, with the exception of Ca which has a minor systematic deficit of 5–13% post-rainfall, there are no consistent temporal variations in major ion concentrations from pre-rainfall to post-rainfall.

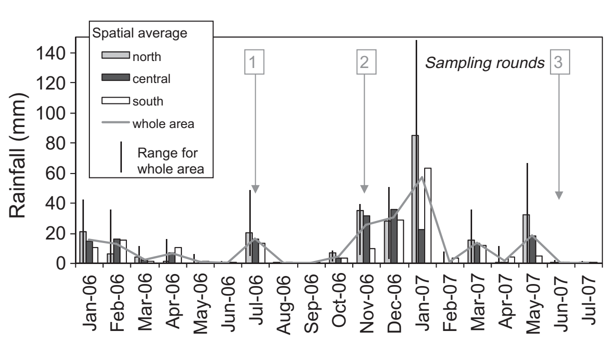

Fig. 4. Rainfall events in the study area. Monthly rainfall indicates large rainfall levels in the northern region during January 2007. Sampling for groundwater and surface water was undertaken twice prior to this event (July and November 2006) and once after this event (June 2007).

TDS contents of groundwater from the Cenozoic aquifer are predominantly comprised of Na and Cl ions; for regional groundwater these are 57–86%, and for Lake Eyre bed and shoreline samples these are 87–98% of the TDS contents. Both the Lake Eyre shoreline and the regional groundwater samples are characterised by the major ion patterns Cl > SO_4 > HCO_3 and Na > Ca > Mg > K (Fig. 7). The relative anion concentrations (Fig. 7) highlights the distinction between groundwater from the Cenozoic aquifer and groundwater from the underlying confined GAB.

The groundwater from within the Lake Eyre bed and surrounding shorelines has TDS values that are higher (26,600–322,000 mg/L) than the regional groundwater from north (4980–52,500 mg/L) and south (7170–28,500 mg/L) of Lake Eyre. However, in both areas to the south and north of Lake Eyre, the groundwater shows no pattern in changing TDS concentrations along groundwater flow paths towards Lake Eyre (Fig. 3b). Therefore, aquifer mineral dissolution reactions with the aquifer substrate are not a dominant process controlling increases in groundwater salinity. There is a general increase in the groundwater TDS content for shallower samples (Fig. 8). Therefore groundwater TDS values may reflect shallow zone processes such as evapotranspiration, vertical mixing and evaporite (e.g. halite and gypsum) dissolution in the unsaturated zone. Major ion analysis of evaporites in the Lake Eyre bed during this study indicates that there is a halite crust at the surface, and in the unsaturated zone there are large gypsum crystals (Table 1). Most groundwater from within the Lake Eyre bed and shoreline is saturated with respect to gypsum (8 of the 10 samples), but only 3 of these are saturated with respect to halite (Table 1). For regional Cenozoic aquifer groundwater, 7 of the 17 samples are saturated with respect to gypsum, and none of these are saturated with respect to halite (Fig. 8). Therefore, if evaporite dissolution were to control increases in groundwater salinity, there is greater potential for the dissolution of halite compared with gypsum. The role of halite dissolution and evapotranspiration controlling groundwater TDS contents are explored further below.

3.3. Cl/Br ratios

Molar Cl/Br ratios of groundwater range from 398 to 10,700. Excluding samples saturated with respect to halite, groundwater Cl/Br ratios during July/November 2006 range from 398 to 1290 and remain relatively constant with increasing Cl concentrations (Fig. 9), indicating that evaporation and/or transpiration is the dominant control on salinity. Cl/Br ratios higher than seawater values (∼650 to 660; Davis et al., 1998) generally indicate there is halite dissolution resulting in the addition of Cl relative to Br. Halite is present as a crust across the Lake Eyre bed and the halite from the salt crust has a Cl/Br ratio of 10,600. There are two groundwater samples saturated with respect to halite from the Lake Eyre bed in the east and west, and both have Cl/Br ratios that indicate halite dissolution has occurred (10,500 and 10,700 respectively; Fig. 9). The Cl/Br ratios from unsaturated zone pore water also show large variations between locations (Table 3). At LE south and LE channel (Fig. 9) the Cl/Br ratio (380–450) indicates that the pore water is saline (Cl: 140–200 g/L) due to evaporation. In comparison, pore water from Lake Eyre east has Cl/Br ratios ranging from 10,000 to 33,000. These Cl/Br ratios are considerably higher than the other pore water samples due to very low Br concentrations of 1.8–6.2 mg/L (0.2–0.6% of the other pore water samples) and moderate Cl concentrations of 16–35 g/L (11–17% of the other pore water samples). Potential reasons for large differences in pore water Cl/Br ratios are discussed further below.

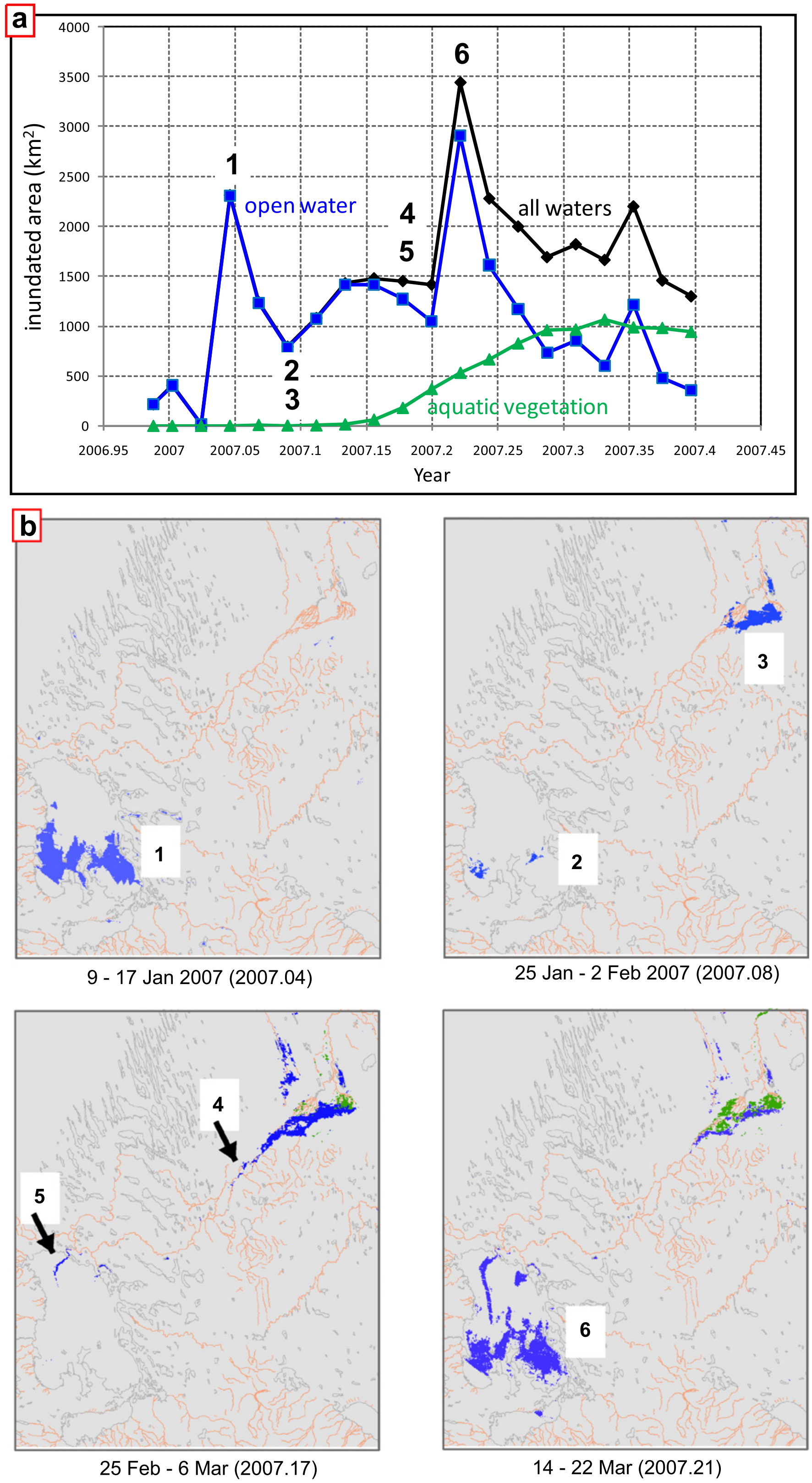

Fig. 5. Inundated areas mapped using MODIS data. (a) Values of inundated areas (all waters) during the flood period, which was calculated using both open water and water under aquatic vegetation. (b) Images of inundated areas (blue = open water; and green = water under aquatic vegetation), where (1) during 9–17 January the local rainfall resulted in ponding in topographic depressions; during 25-January and 2-February (2) the local rainfall dries up and (3) the flood from the headwaters in the northern LEB arrives; during 25-February to 6-March (4) the floodwaters propagate along the Diamantina floodplain and (5) arrive at Lake Eyre; and (6) during 14–22 March Lake Eyre receives the floodwaters. (For interpretation of the references to colour in this figure legend, the reader is referred to the web version of this article.)

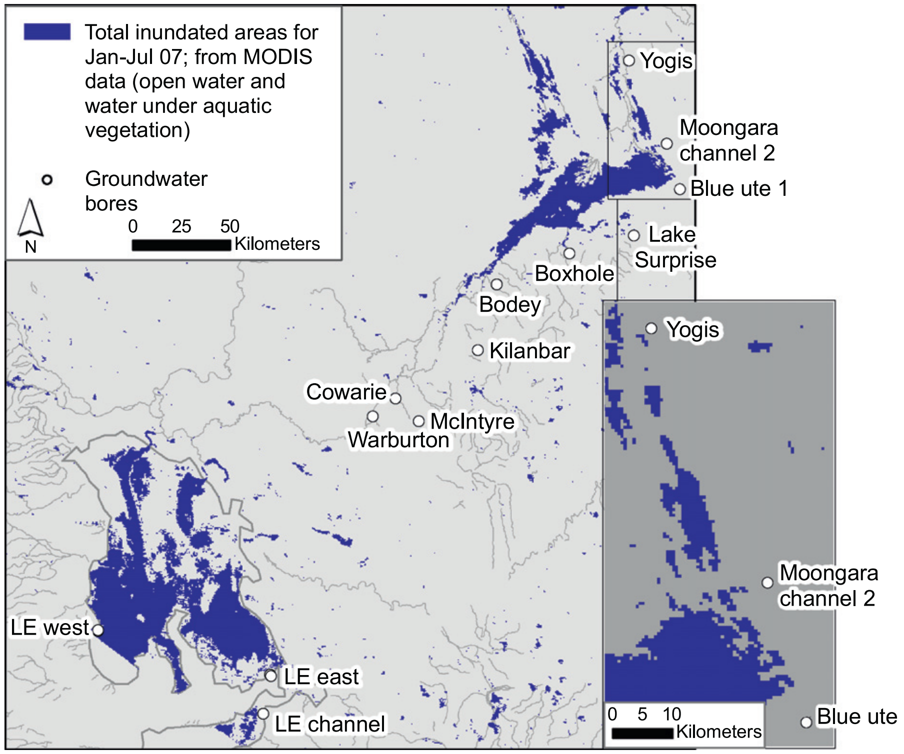

Fig. 6. The total areas inundated during January to July 2007 using MODIS data includes open water, water under aquatic vegetation and very shallow water bodies (extent of Lake Eyre is shown in light grey). Only the Lake Eyre west bore is within the inundated area. The grey insert shows an example of groundwater bores that are located kilometres outside of the floodplain, but this is only evident when shown at a smaller scale.

3.4. Stable isotopes of water

Stable isotope results for surface water (Diamantina River), groundwater from the Cenozoic aquifer, and groundwater from the GAB are presented in Table 2, and pore water results from Lake Eyre are presented in Table 3. When plotted relative to the meteoric water line the $\delta^{18}O$ and δ^2H data indicate that surface water, groundwater in the Cenozoic aquifer and pore water have been evaporated (Fig. 10a). The slope of the least squares fit linear trendlines for all unconfined groundwater (3.85) and surface water (4.39) samples highlight fractionation from the global (GMWL) and local (LMWL) meteoric water lines. Regional groundwater (or groundwater sampled from outside of the Lake Eyre bed and surrounding shorelines) has a slope of 2.97, which is low compared with values usually obtained for evaporating waters (Clark and Fritz, 1997). Implications of this low slope value for discriminating recharge processes and where waters are evaporated in the system are explored further in the discussion.

Groundwater isotope results are compared with modelled trends for evaporation of groundwater at 10%, 30% and 50% humidity (Fig. 10b), and evaporation of groundwater with initial salinity values of 100 and 1000 mmol/L at 30% and 65% humidity (Fig. 10c). These trends were calculated using the approach outlined by Cartwright et al. (2009), which follows work by Craig and Gordon (1986) and Gonfiantini (1986), and calculates stable isotope values of evaporated groundwater ($\delta^{18}O_{evap}$ or δ^2H_{evap}) using the relationship:

$$\delta^{18}O_{evap} = (\delta^{18}O_i - A/B)f^B + A/B \tag{4}$$

where $\delta^{18}O_i$ (or δ^2H_i) is the initial $\delta^{18}O$ (or δ^2H) of recharging rainfall ($\delta^{18}O \sim -9‰$ and $\delta^2H \sim 57‰$), f is the fraction of groundwater that has been evaporated, and A and B are constants defined by:

$$A = \left(\frac{h}{aH_2O_{gw}}\delta^{18}O_v + \Delta\varepsilon + \frac{\varepsilon}{\alpha}\right)\Big/\left(1 - \frac{h}{aH_2O_{gw}} + \frac{\Delta\varepsilon}{1000}\right) \tag{5}$$

$$B = \left(\frac{h}{aH_2O_{gw}} - \frac{\Delta\varepsilon}{1000} - \frac{\varepsilon}{1000\alpha}\right)\Big/\left(1 - \frac{h}{aH_2O_{gw}} + \frac{\Delta\varepsilon}{1000}\right) \tag{6}$$

where h is humidity, aH_2O_{gw} is the activity of groundwater (calculated using Cl concentrations; Cartwright et al., 2009), and $\delta^{18}O_v$ (or δ^2H_v) is the $\delta^{18}O$ (or δ^2H) of water vapour. The $\delta^{18}O$ and δ^2H vapour values were calculated from local precipitation data following the approach described by Jacob and Sonntag (1991). The equilibrium $\delta^{18}O$ and δ^2H values ($\delta^{18}O_{veq}$ and δ^2H_{veq}) of water vapour were calculated using the ^{18}O and ^2H fractionation data of Majoube (1971) and were used to estimate $\delta^{18}O_v$ and δ^2H_v using the following equations:

$$\delta^{18}O_v = (\delta^{18}O_{veq} + 1.4)/0.90 \tag{7}$$

$$\delta^2H_v = \delta^2H_{veq} + 2 \tag{8}$$

This approach is perhaps limited in an arid environment where rainfall levels are low, but in the absence of direct measurements has been deemed acceptable in previous applications (e.g. Gammons et al., 2005; Cartwright et al., 2009).

In equations 5 and 6, α is the equilibrium isotopic fractionation, $\Delta\varepsilon$ is the kinetic enrichment factor (for oxygen = $14.5(1 - h/aH_2O_{gw})$, and for hydrogen = $12.5(1 - h/aH_2O_{gw})$; Gonfiantini, 1986), and ε is the isotope enrichment where

$$\varepsilon = 1000 \times (\alpha - 1) \tag{9}$$

The groundwater stable isotope values lie close to the predicted trends for groundwater evaporated at low humidity (10–50%; Fig. 10b), which is within the range of the annual (3 pm) relative humidity of 17–45 (average 30%; Bureau of Meteorology, 2009).

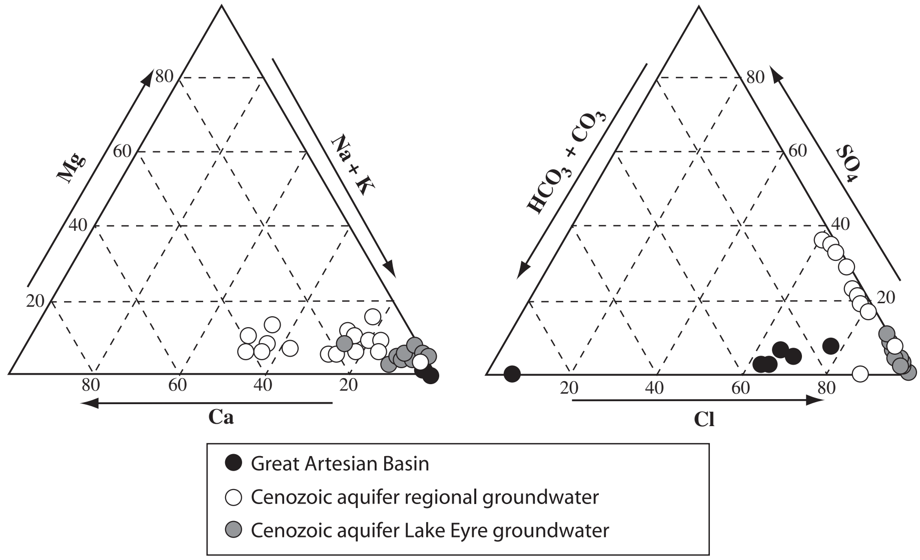

Fig. 7. Ternary diagrams for groundwater in the Cenozoic aquifer (regional areas and within Lake Eyre) compared with groundwater from the GAB.

Fig. 10c illustrates that the regional groundwater has been evaporated from a less saline source (e.g. Cl ~ 100 mmol/L) compared with groundwater from the shoreline at Lake Eyre (e.g. Cl ~ 1000 mmol/L), which is saline due to the evaporation of inflowing regional groundwater. Additionally, the δ^2H activities and Cl concentrations for both the groundwater and pore water sampled from within the Lake Eyre bed lie close to the predicted trend for evaporation of water at a relatively high humidity (e.g. ~65%). As mentioned previously, this is consistent with field observations of the lake, where although rarely inundated, the lake soil profile is wet due to the shallow water table (0–1.1 m; Table 1).

Due to the rainout effect on stable isotope values, a comparison of groundwater with local rainfall stable isotope data can indicate the size of rainfall events predominantly recharging a groundwater system. In the arid Ti-Tree basin, located ~500 km NW of the study area, Harrington et al. (2002) found that groundwater recharge only occurred following very heavy rainfall events (150–200 mm/month). This was evident from the linear extrapolation of groundwater δ^{18}O and δ^2H values to relatively depleted isotope values of amount-weighted mean compositions for different size rainfall events. In this study we use data from IAEA/WMO (2006) at the same rainfall station used by Harrington et al. (2002), Alice Springs which is located at the NW border of the LEB (Fig. 1). The linearly interpolated isotope values for July 2006 and June 2007 groundwater samples are estimated at ~–9‰ and –57‰ for δ^{18}O and δ^2H respectively. At these values the corresponding rainfall levels at the Alice Springs station are >100–150 mm/month (data after Harrington et al., 2002; Fig. 10a). Although, isotope and precipitation data from individual rainfall events is more pertinent in arid regions, there is only monthly data available from the IAEA/WMO (2006). Within the study area, the spatial average of the long-term gridded rainfall data (1900–2006) shows that the highest average monthly rainfall level is 33 mm during January. Therefore groundwater recharge from local rainfall is not a regular occurrence, as it would require rainfall events greater than 3 times average monthly values.

The enrichment of stable isotope values for groundwater from the estimated rainfall values are high (4–15‰ for $\delta^{18}O_{activity}$, and 16–63‰ for $\delta^2H_{activity}$; Fig. 3b), which reflects the extreme arid conditions. The increasing enrichment of δ^2H values with increasing Cl concentrations of groundwater in the Cenozoic aquifer (Fig. 10c) highlights an evaporation control, rather than transpiration, on groundwater salinisation. Shallower groundwater sampled from the Lake Eyre bed and shorelines (depth to water table = 0–1.95 m) shows greater enrichment of stable isotope values (maximum enrichment of $\delta^2H_{activity}$ is 63‰), compared with surrounding regional groundwater with depth to water table ranging from 3.28 to 21.64 m (maximum enrichment of $\delta^2H_{activity}$ is 33‰) (Fig. 10c). The more isotope enriched samples from the Lake Eyre bed and shorelines are also more saline (TDS: 103–322 g/L) (Fig. 10c). The high evaporation rates of groundwater from the Lake Eyre bed and shoreline results in net groundwater discharge, which is the major regional groundwater discharge process for this shallow groundwater system.

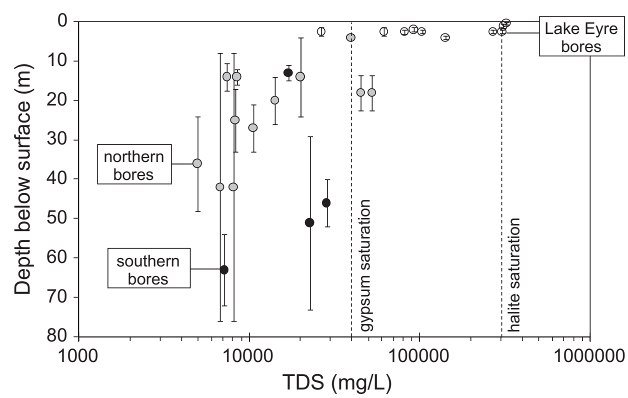

Fig. 8. Increased salinity with decreased depth to sample for groundwater from the north and south of Lake Eyre, and samples from the Lake Eyre shoreline and bed (error bars represent bore screen intervals). Most groundwater with a TDS content >40 g/L are saturated with respect to gypsum, whereas only groundwater with a TDS content >300 g/L are saturated with respect to halite.

3.5. ^{14}C,^{13}C and tritium

The ^{14}C activities of groundwater from the Cenozoic aquifer range from 65.1 to 104.2 pmC (Table 2). ^{14}C activities in the southern hemisphere are similar to those in the northern hemisphere; they decreased from 100 to 97.5 pmC during 1905–1950 (Suess, 1971), increased up to 200 pmC in 1965 (1950–1980: Levin et al., 1995), and exponentially decreased from 135 pmC in 1980

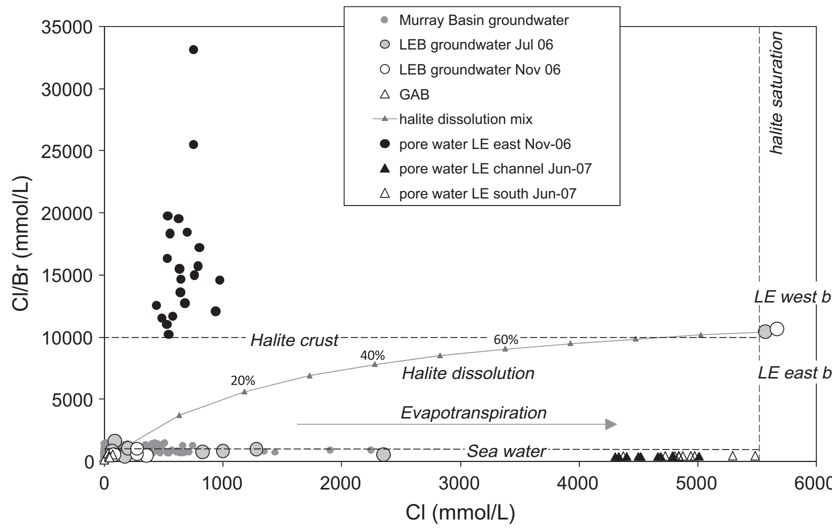

Fig. 9. Cl/Br ratios of most groundwater samples in the Cenozoic remain constant with increasing salinity, similar to results from groundwater in the Murray Basin; where 463 samples from depths ranging 1–235 m showed ranges of Cl/Br between 39 and 1584 (average: 735) (Cartwright et al., 2008; Petrides et al., 2006). The line of halite dissolution represents the addition of water with dissolved halite (Cl/Br = 10,500, Cl = 5570 mmol/L) added to Cenozoic aquifer regional groundwater (Boxhole bore: Cl/Br = 648, Cl = 83 mmol/L), and highlights the trend in Cl/Br ratios with the addition of dissolved halite.

to present (Cartwright et al., 2007b). With the exception of one bore (Cowarie), the ^{14}C activities of groundwater reflect increased mixing with modern rainfall with proximity of groundwater to the surface. ^{14}C activities increase from 70.1 to 104.2 pmC while depth to water table decreases from 21.64 to 1.95 m (Fig. 11a). Although the Cowarie groundwater bore is shallow (sampled at 14 m) and the depth to water table was only 4.73 m deep, the ^{14}C activity is lower than other samples (65.1 pmC). The ^{14}C activity and ^{3}H content for groundwater sampled from the Cowarie bore are discussed further below.

The $\delta^{13}C$ values of groundwater suggest there may be 'dead' carbon (^{14}C-free) in the groundwater, which can decrease activities of ^{14}C (e.g. Clark and Fritz, 1997). The dissolved inorganic carbon (DIC) has a large range in $\delta^{13}C$ values; −16.1‰ to −3.8‰ (median −8.7) (Table 2). There is no marine carbonate in the Cenozoic aquifer, however there are abundant carbonates (detrital or precipitated, inorganically or biologically) in the shallow sediments; the most common are lacustrine facies (Magee et al., 1995). For the same groundwater samples as the radiogenic isotope data, $\delta^{13}C$ values range from −16.1‰ to −12.3‰, but show little correlation to changes in DIC concentrations (3.9–15.4 total C mmol/L). These $\delta^{13}C$ values may reflect dissolution of soil matrix CO_2, or may result from dissolution of freshwater carbonates with a range in $\delta^{13}C$ values (e.g. Cartwright et al., 2007a,b). Changes in Ca (and Ca + Mg) concentrations show little correlation with DIC concentrations, and therefore also suggest that dissolution of calcite or dolomite is minor. Although a minor process in this system, the dissolution of carbonates adds 'dead' carbon to the groundwater, so to account for this a correction of 15% is applied to all samples (e.g. Clark and Fritz, 1997), which is discussed further below.

^{3}H contents range from 0.9 ± 0.2 to 3.5 ± 0.2 TU (Table 2). The high evaporation rates in the study region will impact the tritium activity of the remaining groundwater, however because the changes in absolute isotope ratios are small, the correction is small. For example, Lake Eyre west shows the greatest enrichment of groundwater $\delta^{2}H_{activity}$ values from the estimated rainfall values (enrichment of 29‰). The effect of evaporation on the original value of ^{3}H at 3.5 TU would be an increase by 0.2 TU (Clark and Fritz, 1997), which is the same as the analytical uncertainty (±0.2 TU; Table 2).

The increase of tritium levels in precipitation after the thermonuclear bomb testing (>1960) was to a lesser extent in the southern hemisphere compared to the northern hemisphere (e.g. Doney et al., 1992). ^{3}H values from rainfall collected at the Alice Springs station (Fig. 1) range from 6.2 to 97.2 TU between 1964 and 1976, and 3.1 to 12.8 TU between 1985–1986 (GNIP network; IAEA/WMO, 2006), and in 2007 values were assumed to be ~4.5 TU (similar to precipitation values pre-nuclear test (<1963); Cartwright et al., 2007a,b). Therefore, the ^{3}H data highlights mixing with recent rainfall. Similar to the ^{14}C results, increasing ^{3}H contents (1.3–3.5 TU) with decreased depth to sample (36.5–2.0 m) and decreased depth to water table (21.64–1.95 m) indicate increased mixing with modern rainfall with proximity of groundwater to the surface (Fig. 11b). Again the exception is the Cowarie groundwater bore, which has a relatively low ^{3}H content (0.9 TU) for the sample depth (14 m) and depth to water table (4.73 m). Cowarie is screened in the shale (Fig. 3a); a possible explanation for the lower ^{14}C activity coupled with the lower tritium content is perhaps some mixing with discharging GAB groundwater. In this area GAB groundwater has no detectable tritium and ^{14}C activities are approximately 1.1–1.6 pmC (Mahara et al., 2009). The ^{14}C mixing ratio between groundwater from the Cenozoic aquifer (using the ^{14}C value from a nearby bore: McIntyre) and average GAB groundwater, indicates a 20% input from GAB groundwater at Cowarie. However, all other major ion and stable isotope chemistry results for groundwater at Cowarie is within the range for groundwater from the Cenozoic aquifer, and does not reflect mixing with the GAB. Further work on GAB discharge areas in the LEB is required. The relatively higher ^{3}H values for Lake Eyre west (3.5 TU) compared with Lake Eyre east (2.8 TU; Fig. 11b) correlates well with the inundation mapping that highlights increased inundation of floodwaters at Lake Eyre west (Fig. 6).

By accounting for the radioactive decay and the radiogenic inputs both ^{14}C and ^{3}H have been previously used in other semi-arid regions to estimate renewal rates (e.g. Le Gal La Salle et al., 2001; Cartwright et al., 2007a,b). Following the model outlined by Cartwright et al. (2007a,b), the ^{3}H and ^{14}C results for groundwater in this study are plotted relative to the predicted ^{3}H–^{14}C covariance curve (where $^{14}C_{15\%}$ is the corrected value for dead carbon) for expected values in recharge areas. With the exception of the two samples from Lake Eyre that were sampled from 2 m depth, all groundwater samples lie to the left of the curve (Fig. 11c). These results indicate that in the shallow groundwater system there is mixing between younger water (higher ^{3}H and ^{14}C) and older water (lower ^{3}H and ^{14}C).

Table 3
Locations, Cl and Br concentrations, Cl/Br ratios, and stable isotope results for pore water sampled at 10 cm intervals from the Lake Eyre bed.

Depth (cm)	Date	Location		Cl (mg/L)	Br (mg/L)	Cl/Br ratio	$\delta^2O_{activity}$[a]	$\delta^2H_{activity}$[b]
		Lat	Long				‰ V-SMOW	‰ V-SMOW
Lake Eyre south								
0–10	June-2007	−29.47985	137.1931	190,000	970	450	3.0	63
10–20				170,000	900	420	3.2	61
20–30				190,000	930	450	3.3	60
30–40				170,000	930	420	3.5	61
40–50				170,000	900	430	3.8	61
50–60				170,000	870	430	4.0	62
60–70				180,000	900	440	4.0	61
70–80				170,000	890	440	4.1	62
80–90				170,000	900	440	4.4	64
90–100				150,000	830	420	4.1	63
100–110				170,000	880	440	4.7	65
Lake Eyre channel								
	June-2007	−29.15322	137.70,643	180,000	920	440	6.8	73
10–20				170,000	870	440	7.7	74
20–30				160,000	860	420	7.6	74
30–40				150,000	850	410	7.4	73
40–50				170,000	890	420	7.2	72
50–60				170,000	900	420	7.0	72
60–70				160,000	850	410	6.8	71
70–80				150,000	860	400	7.0	74
80–100				160,000	890	410	7.0	73
100–120				140,000	820	380	6.7	74
Lake Eyre east								
0–10	November-2006	−28.9716	137.7384	19,000	4.2	10,000	9.1	24
10–20				34,000	5.3	15,000	8.9	21
20–30				19,000	2.6	16,000	8.6	17
30–40				33,000	6.2	12,000	8.9	17
40–50				23,000	3.3	16,000	8.7	20
50–60				27,000	4.1	15,000	8.4	13
60–70				21,000	3.9	12,000	8.3	21
70–80				20,000	2.4	18,000	7.9	20
80–90				24,000	4.3	13,000	8.0	17
90–100				23,000	3.8	14,000	8.0	16
100–110				25,000	3.0	18,000	8.8	15
110–120				19,000	3.8	11,000	8.0	12
120–130				27,000	2.4	26,000	7.7	12
130–140				28,000	4.0	16,000	7.8	12
140–150				22,000	2.6	20,000	6.8	12
150–160				19,000	2.2	20,000	7.2	13
160–170				17,000	3.4	12,000	7.5	12
170–180				16,000	2.8	13,000	8.0	14
180–190				23,000	3.5	15,000	7.4	14
190–200				28,000	3.7	17,000	7.4	14
200–210				27,000	1.8	33,000	7 5	13

[a] Measured.
[b] Corrected.

4. Discussion

4.1. Recharge and evaporation processes in an arid environment

Similar to groundwater systems located in other climate regimes (e.g. humid conditions), the controls on groundwater recharge processes and rates in arid regions include local variability due to preferential flow paths, and temporal variability due to changes in land use/land cover and climate (e.g. Simmers, 1997; Scanlon et al., 2006; Leblanc et al., 2009; Favreau et al., 2009). However, within arid regions, groundwater recharge is not a common occurrence since rainfall totals are low and rainfall from individual events can be subject to effective transpiration or evaporation before reaching the saturated zone (Seiler and Gat, 2007). Exceptions to this occur when recharge processes are via ponding of surface water (e.g. Leblanc et al., 2008), when recharge is via sandy aquifers, when there are consecutive heavy rainfall events, or when recharge is via propagating floodwaters (Seiler and Gat, 2007). For example, the Okavango Delta, Botswana, annually floods due to flow from the Okavango river catchment in Angola, and the shallow sandy aquifers are annually recharged by these floodwaters (Wolski and Savenije, 2006). Examples of large semi arid and arid zone endorheic basins are listed in Table 4, with a summary of major recharge and salinisation processes. These examples show that, globally, both focused recharge via surface water flow and diffuse recharge via rainfall are common in most semi arid/arid basins, and the groundwater salinity within each basin greatly varies. In comparison with the other large endorheic basins, at a global scale the LEB has groundwater salinity values in the higher range, similar to groundwater found in the Dead Sea Basin (Table 4). As discussed further below, the groundwater salinity values may be inherently linked to the recharge processes.

In the arid zone of central Australia, the potential recharge processes within the LEB includes direct recharge during local rainfall events, or indirect recharge during the flooding of rivers and creeks. The flooding events within the study area can have exceptionally long travel times, due to both the low river gradient (Diamantina River on average 2.7×10^{-4} m/m; McMahon et al., 2008) and the complex fluvial pathways of anastomising channels covering flood plain widths between 3 and 60 km (Costelloe et al.,

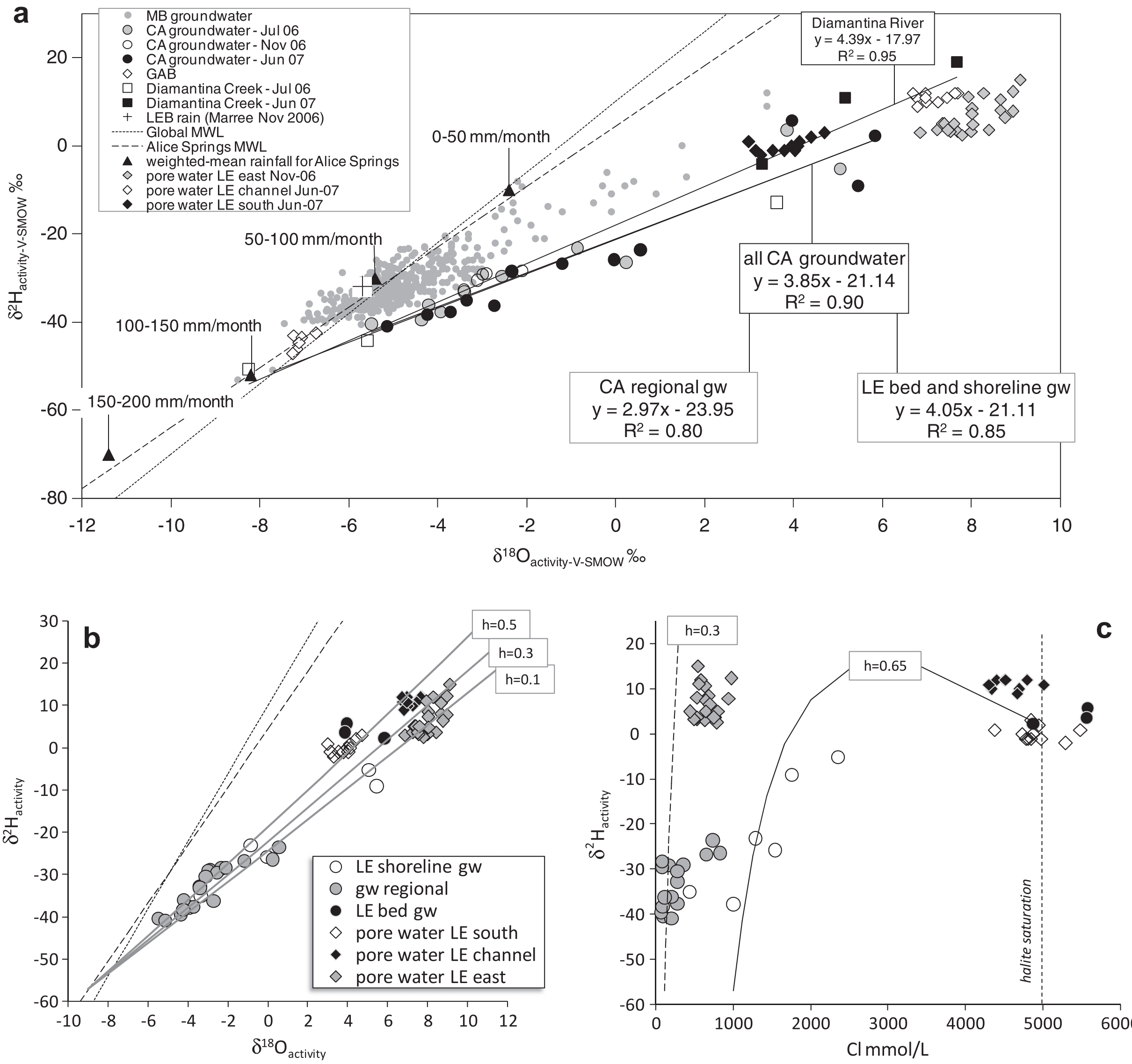

Fig. 10. (a) δ^2H and δ^{18}O activities for groundwater from the Cenozoic aquifer (CA), GAB groundwater, surface water (Diamantina Creek) and one local rain sample (November 2006), compared with the global meteoric water line (GMWL; Craig, 1961) and local MWL (LMWL, Alice Springs station, IAEA/WMO, 2006). Also presented are values for groundwater from the Murray Basin (MB: 356 samples, depths 1–235 m, data from Cartwright et al., 2008; Petrides et al., 2006). The weighted mean isotopic compositions of rainfall events ranging from 0–50 mm/month to >200 mm/month are after data from Harrington et al. (2002). (b) Groundwater and pore water plotted relative to predicted trendlines for evaporation of rainwater at different humidity (10%, 30% and 50%). (c) $\delta^2H_{activity}$ and Cl concentrations of groundwater and pore water indicates the regional Cenozoic aquifer groundwater (gw regional) has evaporation of less saline water (~100 mmol/L) at lower humidity (~30%), compared with groundwater within (LE bed gw) and surrounding (LE shoreline) Lake Eyre, which evaporates more saline water (~1000 mmol/L) at higher humidity (~65%) resulting in high salinity values.

2006). McMahon et al. (2008) hypothesised that the large transmission losses during floods in the LEB (mean 77% water loss in the Diamantina River north of Birdsville) may be due to three factors: (1) termination of fluvial flow paths in low-lying areas; (2) evaporation; and (3) infiltration into the unsaturated zone.

Evaporation can be directly from the groundwater (e.g. Thorburn et al., 1992), and thus is a discharge process, and evaporation can also occur during recharge, either in the unsaturated zone during diffuse groundwater recharge or prior to recharge during surface water flow after large rainfall events. The fractionation of stable isotopes can provide an indication of where in the hydrological pathway the water is predominantly being evaporated. The low slope of 2.97 for regional groundwater may indicate evaporation during diffuse recharge. Gonfiantini (1986) reports evaporated open pan slopes with a minimum of 3.9 at 0% humidity. Lower slopes can be attributed to salinity effects, where at high salinity values (20–50% evaporated seawater) there is decreased fractionation, and reversals in fractionation can occur due to the reduced humidity contrast between the boundary layer and open atmosphere from decreased activity of water (Clark and Fritz, 1997). However, this would result in a low slope only for the more saline groundwater samples. Experimental stable isotope work by Allison (1982) and Barnes and Allison (1983) suggests that arid zone water evaporated through dry soil can also result in a lower slope, compared with evaporation that predominantly occurs from surface water or the water table (slope is typically 4–6). This is due to the increase in thickness of the effective laminar layer above the evaporating surface. Mathematical modelling by Barnes and Allison (1983) indicates that under dry conditions evaporation of water results in a slope that is 30% less than evaporation from wet soils under the same conditions. Interestingly, the slope of 2.97 for regional groundwater is 27% less than the slope of 4.05

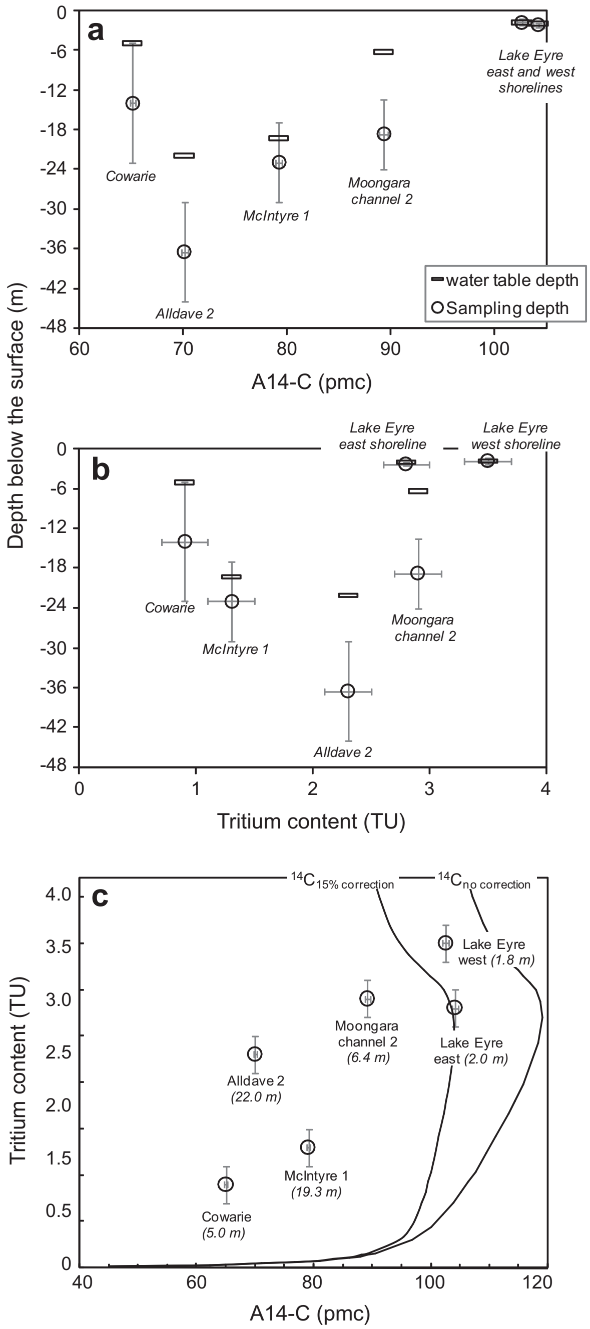

Fig. 11. Depth below the surface to sampling and water table relative to (a) ^{14}C, and (b) ^{3}H. In both graphs the horizontal error bars indicate the analytical accuracy, and the vertical error bars highlight the screened intervals for each bore. (c) Groundwater ^{3}H and ^{14}C relative to the predicted ^{3}H–^{14}C covariance curves for recharge (the curve with no ^{14}C correction and the curve with a correction of 15% to account for dead carbon are presented). Values shown for each sample are the depth to water, which highlight the increased modern recharge input for areas where depth to water is shallow. The error bars highlight the analytical accuracy for ^{3}H and ^{14}C.

for groundwater sampled from the Lake Eyre bed and shoreline, where evaporation occurs under more humid conditions due to the shallow water table. The low slope for the $\delta^{18}O_{activity}$ and $\delta^{2}H_{activity}$ of regional groundwater (Fig. 10a) highlights two processes: (1) groundwater or rainwater is evaporated in the dry unsaturated zone, where rainfall events transport pore water with an evaporated isotope signature; and (2) groundwater is recharged predominantly by diffuse rainfall rather than recharging floodwater. Over the long term, the stable isotope chemistry also suggests that the diffuse recharge is predominantly during periods of heavy local rainfall events (>100–150 mm/month).

The ^{14}C (65.1–104.2 pmC) and ^{3}H (0.9–3.5 TU) data indicate groundwater is receiving modern (decadal) water. The co-variance of ^{3}H contents and ^{14}C activities reflects a shallow groundwater system subject to mixing between old and young water. This may reflect (1) modern recharge mixing with older laterally flowing shallow groundwater, (2) sampling from a groundwater system stratified in response to diffuse recharge, or (3) dual porosity mechanisms controlling the flux of recharge, as was found in the east of the LEB (e.g. Costelloe et al., 2009) and in another semi arid Australian basin (e.g. Cartwright et al., 2007a,b). In dual porosity systems the relatively rapid infiltration of rainfall via fractures results in young water intercepting the water table, which mixes with relatively older groundwater that has more slowly infiltrated via the primary porosity of the matrix. The floodplain areas comprise large areas of cracking clays at the surface, where the cracks provide rapid conduits for infiltration until the clays swell (Wright et al., 1990). In addition to the clay rich shallow aquifers there are also sandstone and shale aquifers that can act as dual porosity mediums.

Other studies have shown that stable isotope values can reflect the mixing between a primary brine formed by evaporation (enriched stable isotope values), and a secondary brine formed by dissolution of halite during infiltration of rainfall (depleted stable isotope values) (e.g. Fontes and Matray, 1993; Dutkiewicz et al., 2000). However in this study, groundwater chemistry shows no evidence of a significant recharge event over the period studied (July-2006 to June-2007), either from flooding or heavy local rainfall events (Fig. 5). Similar to TDS contents (e.g. prior to rainfall TDS: 6760–141,000 mg/L, after rainfall TDS:8120–103,000 mg/L), the groundwater $\delta^{2}H_{activity}$ remain relatively constant prior to ($\delta^{2}H_{activity}$: −41–3‰) and after (−42‰ to 5‰) the rainfall in January-2007 (Fig. 10a), and so do not indicate a recharge event. Therefore, either (1) the transit times are slow and after 6 months we are yet to observe the mixing of groundwater with recharging rainfall; or (2) the relative volume of infiltrating water is low and therefore the change in groundwater chemistry during mixing is minimal. The evaporated unsaturated zone pore water may be transported just by the heavier rains, or by the last rain after a series of events (e.g. Gat, 1995); or (3) evaporation during diffuse recharge results in a similar isotopic fractionation as groundwater values and therefore stable isotopes do not highlight a recharge event. Since major ions also show no systematic temporal variation, the hypothesis (1) or (2) are more plausible. In addition, with the exception of the Lake Eyre west bore, all groundwater samples were located outside of the floodwater area. Transmission losses of the Diamantina River due to infiltration to the shallow groundwater system may still occur but would result in localised groundwater recharge, as was observed for the Lake Eyre west bore.

4.2. Salinisation processes

Although a multitude of hydrologic and geochemical processes can produce saline waters, the evaporation of surface, soil or groundwater is commonly the primary salinisation process in many arid zones (Horita, 2005). Groundwater salinity is intrinsically linked to evaporation during recharge and discharge processes. In the LEB groundwater is saline due to either evaporation during diffuse recharge, or due to groundwater discharge via evaporation. A recent study by Cendón et al. (2010) in the eastern LEB highlighted relatively fresh groundwater lenses (TDS < 5 g/L) in areas where groundwater is locally recharged via waterholes during flood events. Focused recharge is a common phenomenon in many arid zone endorheic basins (Table 4), however the groundwater salinity in these areas is dependent on many

Table 4
Selected examples of large endorheic (semi)arid zone basins.

Basin name	Location	Lake elevation (amsl)	Lake rainfall (mm/yr)	Lake basin surface area (M km^2)	Groundwater salinity (g/L)	Identified groundwater recharge processes	Source
Lake Eyre Basin	Australia	−12	140–260	1.14	5–322	Diffuse rainfall	This study
					0.8–5	Focused via flooding waterholes	Cendón et al. (2010)
Lake Chad Basin	North-central Africa	282	200–400	2.5	0.1–6	Diffuse and focused	Arad and Kafri (1975), Roche (1975), Isiorho et al. (1996), and Olivry et al. (1996)
Lake Titicaca basin	Peru, Bolivia	3800	400	0.19	0.06–12		Coudrain et al. (2001) and Guérin et al. (2001)
Okavango Delta	Botswana	960	450	0.53	0.2–20	Focused	Milzow et al., 2009
Dead sea Basin	Israel/ Jordania/ Palestine	−400	100	0.04	50–340	Diffuse and focused	Yechieli and Sivan (2011)
Aral sea Basin	Central Asia	29	130	1.55	3–23	Diffuse and irrigation water	Shibuo et al. (2006), Johansson et al. (2009), and Benduhn and Renard (2004)
Great Salt Lake basin	Utah, USA	1280	400	0.06	<0.5–10	Diffuse and snow melt	Jones et al. (2009) and Anning et al. (2010)

factors, including the salinity levels of the recharge source. In the Okavango Delta, Botswana, isolated islands of brine swamps results in density driven recharge of saline water (up to 20 g/L) to the underlying aquifers (Milzow et al., 2009).

Although vegetation can be groundwater dependent, and in arid environments vegetation uptake of groundwater can form a significant component of the hydrologic budget (e.g. Lubczynski, 2009), the stable isotope values show that transpiration is not a dominant control on increases in the salinity of the LEB Cenozoic aquifer groundwater (Fig. 10a). This may be due to the desert environment limiting the vegetation types to those species adapted to low transpiration rates e.g. the Eucalyptus coolabah (Costelloe et al., 2008). Regional groundwater has more depleted stable isotope values and lower salinity values (TDS: 5–52 g/L), compared with shallow groundwater beneath the Lake Eyre bed; where the on-going evaporation results in more enriched stable isotope values and greater salinity values (TDS: 27–322 g/L) (Fig. 10c). A previous study has estimated groundwater evaporation/discharge rates (using Cl and Br) from the Lake Eyre bed between 0.9 and 2.8 cm/yr (Ullman, 1985). Additionally, it was found in this study that any GAB groundwater potentially discharging into the Cenozoic aquifer is not significantly altering the major ion and stable isotope chemistry of the shallow groundwater.

The evaporation-driven primary salinisation of groundwater in the arid LEB is distinct from the transpiration-driven primary salinisation of groundwater located in more semi-arid regions of Australia. For example, the Murray Basin (MB) is located closer to the margin of the arid/humid zone (Fig. 1), and high primary salinity values of groundwater in the MB are predominantly due to transpiration rather than evaporation or evaporite dissolution processes (e.g. Cartwright et al., 2008). This is reflected in groundwater with typically lower fractionation of $\delta^{18}O$ and $\delta^{2}H$ from the global MWL (Fig. 10a), and the constant Cl/Br ratios with increasing salinity (Fig. 9). Remnant vegetation in the MB is dominated by species efficient in transpiration and in many regions infiltration rates are low, due to clay-rich soils, which results in effective transpiration of diffuse recharge (Cartwright et al., 2007a,b). Many studies have been devoted to the origin and migration of saline groundwater in the MB due to the high agricultural value of the land, and the adverse impacts agricultural practices have had on salinisation of water resources (e.g. Khan et al., 2008). Land clearance by European settlers during the 19th and 20th centuries, including the change from mallee vegetation to crops, resulted in increased groundwater recharge (e.g. <0.1 to ~3 mm/yr; Allison and Hughes, 1983) and shallower depth to water tables (Allison et al., 1990). Increased evaporation from the shallower water tables now drives secondary salinisation of groundwater in the MB (e.g. Cartwright et al., 2007a,b). Therefore, to date, increased evaporation of groundwater in the MB has resulted from changes in the water budget due to land cover changes, rather than high aridity conditions comparable to the LEB salinity model.

4.3. Bromide in arid environments

Although evaporite minerals are prolific in the lake area, the non-conservative behaviour of Br in pore water limits analysis of the role of halite mineral dissolution and precipitation reactions controlling groundwater salinity. In this study both the Cl and Br concentrations are lower at Lake Eyre east (Cl: 16–35 g/L, Br: 1.8–6.2 mg/L) compared with Lake Eyre south and channel (Cl: 139–200 g/L, Br: 820–970 mg/L; Table 3). In a previous study by Ullman (1985), the pore water results were 149–181 g/L for Cl, and 58–110 mg/L for Br concentrations sampled to 0.6 m depth in a similar location to Lake Eyre east. The relatively low Cl and Br concentrations at Lake Eyre east from our study may result from a dilution process. The presence of interspersed layers of sand with mud within the Lake Eyre profile (e.g. Ullman, 1985) suggests that non-uniform mixing with shallow groundwater occurs across Lake Eyre. However, at Lake Eyre east the Br concentrations are significantly lower compared with Cl concentrations resulting in high Cl/Br ratios (10,300–33,200), which cannot be accounted for by the dissolution of halite (Fig. 9). This indicates there is a relative loss of Br from solution.

In many systems, Br behaves relatively conservatively, and has therefore been widely used in hydrogeological studies as an injected tracer for determining groundwater recharge (e.g. Scanlon et al., 2002), groundwater/surface water interaction (Cartwright et al., 2009) and to investigate sources of increased salinisation when compared with changes in Cl concentrations (e.g. Kloppmann et al., 2001; Casanova et al., 2001; Faye et al., 2005; Labus, 2005). However, processes exist in the natural environment that can result in changes in the Br relative to Cl concentrations. The low Br concentrations in the pore water, may be due to (1) adsorption on surfaces modified by organic matter (e.g. Gerritse and George, 1988) or iron and manganese oxides (e.g. Wood and Sanford, 2007); (2) uptake by plants during transpiration (e.g.

Kung, 1990; Parsons et al., 2004), however there is no vegetation on the lake bed; (3) incorporation into halite during precipitation, but this only takes up small amounts of Br to replace Cl and the pore water at Lake Eyre east was below halite saturation; or (4) flux of Br to the atmosphere. Recent studies have shown there are significant levels of Br released to the free troposphere away from polar regions, via autocatalytic oxidation of sea salt halides or degradation of organic halogen compounds (e.g. Platt and Hönninger, 2003). In regions of high evaporation rates, recent studies have observed decreases in Br concentrations relative to other conservative ions in salt pans (e.g. Hönninger et al., 2004), surface water (e.g. Risacher et al., 2006), and groundwater (e.g. Wood and Sanford, 2007), and have related the decrease in concentrations to the atmospheric flux of Br. In arid environments, if the residence time is sufficient, there can be Br flux directly from the brine to the atmosphere; otherwise because of the greater surface area of salt efflouresences, in less time there can be significant flux of Br from the salt to the atmosphere (e.g. Risacher et al., 2006). As suggested by Wood and Sanford (2007), further work to help constrain controls on the non-conservative behaviour of Br may include analysis of δ^{81}Br. The non-conservative behaviour of Br has important implications for the use of Cl/Br ratios in hydrological investigations of arid environments. For example determining dominant processes controlling the salinisation of water resources (e.g. Cartwright et al., 2007a,b; Druhan et al., 2008), or for estimating discharge rates (e.g. Ullman, 1985).

5. Conclusions

In a relatively unexplored shallow groundwater system in the central Australian desert, recharge and salinity processes across an endorheic basin were investigated. In the absence of sufficient on-ground physical groundwater monitoring data, groundwater chemistry, particularly stable isotope chemistry, proved valuable in providing hydrogeological information on long term and dominant processes in the remote and arid region. Stable isotope (δ^{18}O and δ^{2}H) data showed that groundwater is principally recharged during larger and intense rainfall events. The stable isotopes also indicate that over longer timeframes, groundwater recharge is predominantly via diffuse processes rather than infiltration of floodwaters, but these results may locally vary with distance from the floodplain. Radiogenic isotope (^{14}C and ^{3}H) data reflect an older shallow groundwater system subject to mixing with recently (post-1951) infiltrated water. The geochemical data were unable to highlight groundwater recharge from a single flood event in 2007 (shown using remote sensing data); however this does not preclude the process.

Groundwater outside of Lake Eyre has high salinity values (TDS: 5–52 g/L) associated with low infiltration and high evaporations rates. During diffuse recharge, effective evaporation of infiltrating rainfall results in saline water which is transported to the saturated zone. Groundwater flow paths terminate at Lake Eyre, where the shallow groundwater is exposed to on-going evaporation. Therefore, the increased salinity levels of groundwater within Lake Eyre (TDS: 27–322 g/L) are linked to groundwater discharge via evaporation. The salinity model of the LEB is driven by high evaporation rates during groundwater recharge and discharge, similar to many arid basins globally. This is distinct from the Murray Basin (Australia) located in a semi-arid climate; where primary salinity is transpiration-driven and secondary salinisation of groundwater due to evaporation has mostly resulted from rising water tables linked with land cover changes.

Defining hydrogeological processes in a remote region, over a large area, with limited background hydrogeological data inevitably raises more questions than it answers. An example of the large spatial heterogeneity present within this study area are the variations in Cl/Br ratios of pore water sampled from three locations across Lake Eyre, and the non-conservative behaviour of Br at one of these sights. The current assessment of the recharge and salinity controls on groundwater in such an environment should be subject to reworking.

Acknowledgements

This study was funded by the Australian Research Council (ARC, 2005–2008). The authors also wish to acknowledge help from Bob Paull, Chris Grant, Guillaume Ramillien, Jean-Francois Creteaux and Paul Pavlik for fieldwork, and advice from Elizabeth Irvine and Justin Costelloe (University of Melbourne). The authors would also like to thank the reviewers and associate editor for their constructive comments during the review process.

References

Al-Katheeri, E.S., 2008. Towards the establishment of water management in Abu Dhabi Emirate. Water Resour. Manage. 22, 205–215.
Allison, G.B., 1982. The relationship between δ^{18}O and deuterium in water in sand columns undergoing evaporation. J. Hydrol. 55, 163–169.
Allison, G.B., Hughes, M.W., 1983. The use of natural tracers as indicators of soil–water movement in a temperate semi-arid region. J. Hydrol. 60, 157–173.
Allison, G.B., Cook, P.G., Barnett, S.R., Walker, G.R., Jolly, I.D., Hughes, M.W., 1990. Land clearance and river salinisation in the western Murray Basin, Australia. J. Hydrol. 119, 1–20.
Allison, G.B., Gee, G.W., Tyler, S.W., 1994. Vadose-zone techniques for estimating groundwater recharge in arid and semiarid regions. Soil Sci. Soc. Am. 58, 6–14.
Anning, D.W., Bauch, N.J., Gerner, S.J., Flynn, M.E., Hamlin, S.N., Moore, S.J., Schaefer, D.H., Anderholm, S.K., Spangler, L.E., 2010, Dissolved solids in basin-fill aquifers and streams in the Southwestern United States: US Geological Survey Scientific Investigations Report 2006-5315, v.1.1., 168 p.
Arad, A., Kafri, U., 1975. Geochemistry of groundwaters in the Chad basin. J. Hydrol. 25, 105–127.
Barnes, C.J., Allison, G.B., 1983. The distribution of deuterium and ^{18}O in dry soils, 1. Theory. J. Hydrol. 60, 141–156.
Benduhn, F., Renard, P., 2004. A dynamic model of the Aral Sea water and salt balance. J. Marine Syst. 47, 35–50.
Bobba, A.G., Bukata, R.P., Jerome, J.H., 1992. Digitally processed satellite data as a tool in detecting potential groundwater flow systems. J. Hydrol. 131, 25–62.
Bukata, R.P., 2005. Satellite Monitoring of Inland and Coastal Water Quality: Retrospection, Introspection, Future Directions. Taylor and Francis, New York.
Cartwright, I., Weaver, T.R., Fifield, L.K., 2006. Cl/Br ratios and environmental isotopes as indicators of recharge variability and groundwater flow: an example from the southeast Murray Basin, Australia. Chem. Geol. 231, 38–56.
Cartwright, I., Hannam, K., Weaver, T.R., 2007a. Constraining flow paths of saline groundwater at basin margins using hydrochemistry and environmental isotopes: Lake Cooper, Murray Basin, Australia. Aust. J. Earth Sci. 54, 1103–1122.
Cartwright, I., Weaver, T.R., Stone, D., Reid, M., 2007b. Constraining modern and historical recharge from bore hydrographs, ^{3}H, ^{14}C, and chloride concentrations: Applications to dual-porosity aquifers in dryland salinity areas, Murray Basin, Australia. J. Hydrol. 332, 69–92.
Cartwright, I., Weaver, T.R., Tweed, S.O., 2008. Integrating physical hydrogeology, hydrochemistry, and environmental isotopes to constrain regional groundwater flow: southern Riverine Province, Murray Basin, Australia. In: Carillo, J., Ortega, G. (Eds.), Groundwater Flow Understanding from Local to Regional Scale. Taylor & Francis, pp. 105–133 (Chapter 4).
Cartwright, I., Hall, S., Tweed, S., Leblanc, M., 2009. Geochemical and isotopic constraints on the interaction between saline lakes and groundwater in southeast Australia. Hydrogeol. J. doi:10.1007/s10040-009-0492-5.
Casanova, J., Négrel, Ph., Kloppmann, W., Aranyossy, J.F., 2001. Origin of deep saline groundwaters in the Vienne granitic rocks (France): constraints inferred from boron and strontium isotopes. Geofluids 1, 91–102.
Cendón, D.I., Larsen, J.R., Jones, B.G., Nanson, G.C., Rickleman, D., Hankin, S.I., Pueyo, J.J., Maroulis, J., 2010. Freshwater recharge into a shallow saline groundwater system, Cooper Creek floodplain, Queensland, Australia. Journal of Hydrology 392, 150–163.
Clark, I., Fritz, P., 1997. Environmental Isotopes in Hydrogeology. Lewis Publishers.
Collins, A.G., 1975. Geochemistry of oilfield waters. Developments in Petroleum Science 1. Elsevier, Amsterdam.
Coplen, T.B., 1988. Normalization of oxygen and hydrogen isotope data. Chem. Geol. 72, 293–297.
Costelloe, J.F., Grayson, R.B., McMahom, T.A., 2006. Modelling streamflow in a large anastomosing river of the arid zone, Diamantina River, Australia. J. Hydrol. 323, 138–153.
Costelloe, J.F., Shield, A., Grayson, R.B., McMahon, T.A., 2007. Determining loss characteristics of arid zone river waterbodies. River Res. Appl. 23, 715–731.

Costelloe, J.F., Payne, E., Woodrow, I.E., Irvine, E.C., Andrew, W., Western, A.W., Leaney, F.W., 2008. Water sources accessed by arid zone riparian trees in highly saline environments, Australia. Oecologia 156, 43–52.

Costelloe, J.F., Irvine, E.C., Western, A.W., Herczeg, A.L., 2009. Groundwater recharge and discharge dynamics in an arid-zone ephemeral lake system, Australia. Limnol. Oceanogr. 54 (1), 86–100.

Coudrain, A., Talbi, A., Ledoux, E., Loubet, M., Vacher, J., Ramirez, E., 2001. Subsurface transfer of chloride after a lake retreat in the Central Andes. Ground Water 39 (5), 751–759.

Craig, H., 1961. Isotopic variations in meteoric waters. Science 133, 1702–1703.

Craig, H., Gordon, L.I., 1986. Deuterium and oxygen-18 variations in the ocean and atmosphere. In: Tongiorgi, E. (Ed.), Stable Isotopes in Oceanographic Studies and Palaeotemperatures. Consiglio Nazionale Delle Ricerche Laboratorio di Geologia Nucleare, Pisa, pp. 9–130.

Dahan, O., Tatarsky, B., Enzel, Y., Kulls, C., Seely, M., Benito, G., 2008. Dynamics of flood water infiltration and ground water recharge in hyperarid desert. Ground Water 46 (3), 450–461.

Davis, S.N., Whittemore, D.O., Fabryka-Martin, J., 1998. Uses of chloride/bromide in studies of potable water. Ground Water 36, 338–351.

Doney, S.C., Glover, D.M., Jenkins, W.J., 1992. A model function of the global bomb tritium distribution in precipitation, 1960–1986. J. Geophys. Res. 97 (C4), 5481–5492.

Druhan, J.L., Hogan, J.F., Eastoe, C.J., Hibbs, B.J., Hutchison, W.R., 2008. Hydrogeologic controls on groundwater recharge and salinization: a geochemical analysis of the northern Hueco Bolson aquifer, Texas, USA. Hydrogeol. J. 16, 281–296.

Dutkiewicz, A., Herczeg, A.L., Dighton, J.C., 2000. Past changes to isotopic and solute balances in a continental playa: clues from stable isotopes of lacustrine carbonates. Chem. Geol. 165, 309–329.

Edmunds, W.M., Gaye, C.B., 1994. Estimating the spatial variability of groundwater recharge in the Sahel using chloride. J. Hydrol. 156, 47–59.

Engman, E.T., Gurney, R.J., 1991. Remote Sensing in Hydrology. Chapman and Hall, London.

Favreau, G., Leduc, C., Marlin, C., Dray, M., Taupin, J.-D., Massault, M., Le Gal La Salle, C., Babic, M., 2002. Estimate of recharge of a rising water table in semiarid Niger from ^{3}H and ^{14}C Modeling. Ground Water 40 (2), 144–151.

Favreau, G., Cappelaere, B., Massuel, S., Leblanc, M., Boucher, M., Boulain, N., Leduc, C., 2009. Land clearing, climate variability, and water resources increase in semiarid southwest Niger: a review. Water Resour. Res. 45, W00A16. doi:10.1029/2007WR006785.

Faye, S., Maloszewski, P., Stichler, W., Trimborn, P., Cissé Faye, S., Gaye, C.B., 2005. Groundwater salinization in the Saloum (Senegal) delta aquifer: minor elements and isotopic indicators. Sci. Total Environ. 343 (1–3), 243–259.

Fontes, J.Ch., Matray, J.M., 1993. Geochemistry and origin of formation brines from the Paris Basin, France. 1. Brines associated with Triassic salts. Chem. Geol. 109, 149–175.

Gammons, C.H., Poulson, S.R., Pelicori, D.A., Reed, P.J., Roesler, A.J., Petrescu, E.M., 2005. The hydrogen and oxygen isotopic composition of precipitation, evaporated mine water, and riverwater in Montana, USA. J. Hydrol. 328, 319–330.

Gat, J.R., 1995. The relationship between the isotopic composition of precipitation, surface runoff and groundwater for semiarid and arid zones. Application of tracers in Arid Zone Hydrology (Proceedings of the Vienna Symposium, August 1994), vol. 232. IAHS Publication, pp. 409–416.

Gates, J.B., Edmunds, W.M., Ma, J., Scanlon, B.R., 2008. Estimating groundwater recharge in a cold desert environment in northern China using chloride. Hydrogeol. J. 16 (5), 893–910.

Gerritse, R.G., George, R.J., 1988. The role of soil organic matter in the geochemical cycling of chloride and bromide. J. Hydrol. 101, 83–85.

Gonfiantini, R., 1986. Environmental isotopes in lake studies. In: Fritz, P., Fontes, J.C. (Eds.), Handbook of Environmental Isotope Geochemistry. The Terrestrial Environment, vol. 2. Elsevier, Amsterdam, pp. 113–186.

Guérin, R., Descloitres, M., Coudrain, A., Talbi, A., Gallaire, R., 2001. Geophysical surveys for identifying saline groundwater in the semi-arid region of the central ltiplano, Bolivia. Hydrol. Process. 15, 3287–3301.

Harrington, G.A., Cook, P.G., Herczeg, A.L., 2002. Spatial and temporal variability of groundwater recharge in central Australia: a tracer approach. Ground Water 40 (5), 518–528.

Herczeg, A.L., Torgersen, T., Chivas, A.R., Habermehl, M.A., 1991. Geochemistry of ground waters from the Great Artesian Basin, Australia. J. Hydrol. 126, 225–245.

Herczeg, A.L., Dogramaci, S.S., Leaney, F.W.J., 2001. Origin of dissolved salts in a large, semi-arid groundwater system: Murray Basin, Australia. Mar. Freshwater Res. 52, 41–52.

Hesse, P.P., Magee, J.W., van der Kaars, S., 2004. Late Quaternary climates of the Australian arid zone: a review. Quat. Int. 118–119, 87–102.

Hoffmann, J., 2005. The future of satellite remote sensing in hydrogeology. Hydrogeol. J. 13, 247–250.

Hönninger, G., Bobrowski, N., Palenque, E.R., Torrez, R., Platt, U., 2004. Reactive bromine and sulfur emission at salar de Uyuni, Bolivia. Geophys. Res. Lett. 31. doi:10.1029/2003GL018818.

Horita, J., 1989. Analytical aspects of stable isotopes in brines. Chem. Geol., Isotope Geosci. Sec. 79, 107–112.

Horita, J., 2005. Saline waters. In: Aggarwal, P.K., Gat, J.R., Froehlich, K.F.O. (Eds.), Isotopes in the Water Cycle: Past, Present and Future of a Developing Science, pp. 271–287 (Chapter 17).

Hutchison, W.R., Hibbs, B.J., 2008. Ground water budget analysis and cross-formational leakage in an arid basin. Ground water 43 (3), 384–395.

IAEA/WMO, 2006. Global Network of Isotopes in Precipitation. The GNIP Database. <http://isohis.iaea.org>.

Isiorho, S.A., Matisoff, G., When, K.S., 1996. Seepage relationships between Lake Chad and the Chad Aquifers. Ground Water 34 (5), 819–826.

Jackson, T.J., 2002. Remote sensing of soil moisture: implications for groundwater recharge. Hydrogeol. J. 10, 40–51.

Jacob, H., Sonntag, C., 1991. An 8-year record of the seasonal variation of ^{2}H and ^{18}O in atmospheric water vapor and precipitation at Heidelberg, Germany. Tellus 43B, 291–300.

Johansson, O., Aimbetov, I., Jarsjö, J., 2009. Variation of groundwater salinity in the partially irrigated Amudarya River delta, Uzbekistan. J. Marine Syst. 76, 287–295.

Johnson, B.J., Miller, G.H., Magee, J.W., Gagan, M.K., Fogel, M.L., Quay, P.D., 2005. Carbon isotope evidence for an abrupt reduction in grasses coincident with European settlement of Lake Eyre, South Australia. Holocene 15 (6), 888–896.

Jones, B.F., Naftz, D.L., Spencer, R.J., Charles, G., Oviatt, C.G., 2009. Geochemical evolution of Great Salt Lake, Utah, USA. Aquat. Geochem. 15, 95–121.

Justice, C.O., Townshend, J.R.G., Vermote, E.F., Masuoka, E., Wolfe, R.E., El Saleous, N., Roy, D.P., Morisette, J.T., 2002. An overview of MODIS Land data processing and product status. Remote Sens. Environ. 83 (1–2), 3–15.

Khan, S., Rana, T., Hanjra, M.A., 2008. A cross disciplinary framework for linking farms with regional groundwater and salinity management targets. Agric. Water Manage. 95, 35–47.

Kingsford, R.T., Porter, J.L., 1993. Waterbirds of Lake Eyre, Australia. Biol. Conserv. 65, 141–151.

Kloppmann, W., Négrel, Ph., Casanova, J., Klinge, H., Schelkes, K., Guerrot, C., 2001. Halite dissolution derived brines in the vicinity of a Permian salt dome (N German Basin). Evidence from boron, strontium, oxygen, and hydrogen isotopes. Geochim. Cosmochim. Acta 65 (22), 4087–4101.

Kotwicki, V., Allan, R., 1998. La Niña de Australia—contemporary and palaeo-hydrology of Lake Eyre. Palaeogeogr. Palaeoclimatol. Palaeoecol. 144, 265–280.

Kreig, G.W., Callen, R.A., Gravestock, D.I., Gatehouse, C.G., 1990. Geology. In: Tyler, M.J., Twidale, C.R., Davies, M., Wells, C.B. (Eds.), Natural History of the North East Deserts. Royal Society of Australia Inc., pp. 1–26 (Chapter 1).

Kung, K.J.-S., 1990. Influence of plant uptake on the performance of bromide tracer. Soil Sci. Soc. Am. J. 54, 975–979.

Labus, K., 2005. Origin of groundwater mineralization in coarse-grained lower Badenian aquifer in the Czech part of the Upper Silesian Coal Basin. Geol. Quart. 49 (1), 75–82.

Le Gal La Salle, C., Marlin, C., Leduc, C., Taupin, J.D., Massault, M., Favreau, G., 2001. Renewal rate estimation of groundwater based on radioactive tracers (^{3}H, ^{14}C) in an unconfined aquifer in a semi-arid area, Iullemeden Basin, Niger. J. Hydrol. 254, 145–156.

Leblanc, M., Razack, M., Dagorne, D., Mofor, L., Jones, C., 2003a. Application of Meteosat thermal data to map soil infiltrability in the central part of the Lake Chad basin, Africa. Geophys. Res. Lett. 30 (19). doi:10.1029/2003GL018094.

Leblanc, M., Leduc, C., Razack, M., Lemoalle, J., Dagorne, D., Mofor, L., 2003b. Application of remote sensing and GIS for groundwater modelling of large semiarid areas: example of the Lake Chad Basin, Africa. In: Hydrology of Mediterranean and Semiarid Regions. IAHS (Red Books Series), vol. 278. IAHS Press Centre for Ecology and Hydrology, Wallingford. Publ., pp. 186–192.

Leblanc, M., Favreau, G., Tweed, S., Leduc, C., Razack, M., Mofor, L., 2007. Remote sensing for groundwater modelling in large semiarid areas: Lake Chad Basin, Africa. Hydrogeol. J. (Special issue on Remote Sensing and GIS in Hydrogeology). 15, 97–100.

Leblanc, M., Favreau, G., Massuel, S., Tweed, S., Loireau, M., Cappelare, B., 2008. Land clearance and hydrological change in the Sahel. Global Planet. Change 61 (3–4), 135–150.

Leblanc, M.J., Tregoning, P., Ramillien, G., Tweed, S.O., Fakes, A., 2009. Basin-scale, integrated observations of the early 21st century multiyear drought in southeast Australia. Water Resour. Res. 45, W04408. doi:10.1029/2008WR007333.

Leblanc, M., Lemoalle, J., Bader, J.-C., Tweed, S., Mofor, L., 2011. Thermal remote sensing of water under flooded vegetation: new observations of inundation patterns for the 'Small' Lake Chad. Journal of Hydrology. doi:10.1016/j.jhydrol.2011.04.023.

Levin, I., Graul, R., Trivett, N.B.A., 1995. Long term observations of atmospheric CO_2 and carbon isotopes at continental sites in Germany. Tellus 47B, 23–34.

Li, R.-R., Kaufman, Y.J., Gao, B.-C., Davis, C.O., 2003. Remote sensing of suspended sediments and shallow coastal waters. IEEE Trans. Geosci. Remote Sens. 41 (3), 559–566.

Love, A.J., Herczeg, A.L., Sampson, L., Cresswell, R.G., Fifield, L.K., 2000. Sources of chloride and implications for 36Cl dating of old groundwater, southwestern Great Artesian Basin, Australia. Water Resour. Res. 36 (6), 1561–1574.

Lubczynski, M.W., 2009. The hydroegological role of trees in water-limited environments. Hydrogeol. J. 17, 247–259.

Lunetta, R.S., Knight, J.F., Ediriwickrema, J., Lyon, J.G., Worthy, L.D., 2006. Land-cover change detection using multi-temporal MODIS NDVI data. Remote Sens. Environ. 105, 142–154.

Lyon, J.G., Yuan, D., Lunetta, R.S., Elvidge, C.D., 1998. A change detection experiment using vegetation indices. Photogram. Eng. Remote Sens. 64 (2), 143–150.

Ma, J.Z., Wang, X.S., Edmunds, W.M., 2005. The characteristics of ground-water resources and their changes under the impacts of human activity in the arid Northwest China—a case study of the Shiyang River Basin. J. Arid Environ. 61, 277–295.

Magee, J.W., Bowler, J.M., Miller, G.H., Williams, D.L.G., 1995. Stratigraphy, sedimentology, chronology and palaeohydrology of Quaternary lacustrine deposits at Madigan Gulf, Lake Eyre, South Australia. Palaeogeogr. Palaeoclimatol. Palaeoecol. 113, 3–42.

Mahara, Y., Habermehl, M.A., Hasegawa, T., Nakata, K., Ransley, T.R., Hatano, T., Mizuochi, Y., Kobayashi, H., Ninomiya, A., Senior, B.R., Yasuda, H., Ohta, T., 2009. Groundwater dating by estimation of groundwater flow velocity and dissolved 4He accumulation rate calibrated by 36Cl in the Great Artesian Basin, Australia. Earth Planet. Sci. Lett. doi:10.1016/j.epsl.2009.07.034.

Majoube, M., 1971. Oxygène-18 et en deutérium entre l'eau et sa vapeur (fractionation of oxygen-18 and deuterium between water and vapour). J. Chim. Phys. 10, 1423–1436.

Martin, H.A., 2006. Cenozoic climatic change and the development of the arid vegetation in Australia. J. Arid Environ. 66, 533–563.

Massuel, S., Favreau, G., Descloitres, M., Le Troquer, Y., Albouy, Y., Cappelaere, B., 2006. Deep infiltration through a sandy alluvial fan in semiarid Niger inferred from electrical conductivity survey, vadose zone chemistry and hydrological modeling. Catena 67, 105–118.

McMahon, T.A., Murphy, R.E., Peel, M.C., Costelloe, J.F., Chiew, F.H.S., 2008. Understanding the surface hydrology of the Lake Eyre Basin: Part 2 – Streamflow. J. Arid Environ. 72, 1869–1886.

Milzow, C., Kgotlhang, L., Bauer-Gottwein, P., Meier, P., Kinzelbach, W., 2009. Regional review: the hydrology of the Okavango Delta, Botswana—processes, data and modelling. Hydrogeol. J. 17, 1297–1328.

Moussavi-Harami, R., Alexander, E., 1998. Tertiary stratigraphy and tectonics, Eromanga Basin region. MESA J. 8, 32–36.

Mudd, G.M., 2000. Mound springs of the Great Artesian Basin in South Australia: a case study from Olympic Dam. Environ. Geol. 39 (5), 463–476.

Olivry, J.C., Chouret, A., Vuillaume, G., Lemoalle, J., Bricquet, J.P., 1996. Hydrologie du Lac Tchad. ORSTOM, Paris, 259 p.

Parkhurst, D.L., Appelo, C.A.J., 1999. User's guide to PHREEQC (version 2): a computer program for speciation, batch-reaction, one-dimensional transport, and inverse geochemical calculations. US Geological Survey Water-Resources Investigations Report 99-4259, US Geol. Surv., Reston, Va.

Parsons, D.F., Hayashi, M., van der Kamp, G., 2004. Infiltration and solute transport under a seasonal wetland: bromide tracer experiments in Saskatoon, Canada. Hydrol. Process. 18 (11), 2001–2027.

Petrides, B., Cartwright, I., Weaver, T.R., 2006. The evolution of groundwater in the Tyrrell catchment, south-central Murray Basin, Victoria, Australia. Hydrogeol. J. 14, 1522–1543.

Pirlo, M.C., 2004. Hydrogeochemistry and geothermometry of thermal groundwaters from the Birdsville Track Ridge, Great Artesian Basin, South Australia. Geothermics 33, 743–774.

Platt, U., Hönninger, G., 2003. The role of halogen species in the troposphere. Chemosphere 52, 325–338.

Puckridge, J.T., Walker, K.F., Costelloe, J.F., 2000. Hydrological persistence and the ecology of dryland rivers. Regul. Rivers: Res. Manage. 16, 385–402.

Rabemanana, V., Violette, S., de Marsily, G., Robain, H., Deffontaines, B., Andrieux, P., Bensimon, M., Parriaux, A., 2005. Origin of the high variability of water mineral content in the bedrock aquifers of Southern Madagascar. J. Hydrol. 310, 143–156.

Radke, B.M., Ferguson, J., Cresswell, R.G., Ransley, T.R., Habermehl, M.A., 2000. Hydrochemistry and Implied Hydrodynamics of the Cadna-owie-Hooray Aquifer, Great Artesian Basin, Australia. Bureau of Rural Sciences, Canberra.

Risacher, F., Fritz, B., Alonso, H., 2006. Non-conservative behavior of bromide in surface waters and brines of Central Andes: a release into the atmosphere. Geochim. Cosmochim. Acta 70, 2143–2152.

Roche, M.-A., 1975. Geochemistry and natural ionic and isotopic tracing; two complementary ways to study the natural salinity regime of the hydrological system of Lake Chad. J. Hydrol. 26 (1–2), 153–171.

Roshier, D.A., Whetton, P.H., Allan, R.J., Robertson, A.I., 2001. Distribution and persistence of temporary wetland habitats in arid Australia in relation to climate. Aust. Ecol. 26, 371–384.

Salama, R., Tapley, I., Ishii, T., Hawkes, G., 1994. Identification of areas of recharge and discharge using Landsat-TM satellite imagery and aerial photography mapping techniques. J. Hydrol. 162, 119–141.

Scanlon, B.R., Healy, R.W., Cook, P.G., 2002. Choosing appropriate techniques for quantifying groundwater recharge. Hydrogeol. J. 10, 18–39.

Scanlon, B.R., Keese, K.E., Flint, A.L., Flint, L.E., Gaye, C.B., Edmunds, W.M., Simmers, I., 2006. Global synthesis of groundwater recharge in semiarid and arid regions. Hydrol. Process. 20, 3335–3370.

Scanlon, B.R., Stonestrom, D.A., Reedy, R.C., Leaney, F.W., Gates, J., Cresswell, R.G., 2009. Inventories and mobilization of unsaturated zone sulfate, fluoride, and chloride related to land use change in semiarid regions, southwestern United States and Australia. Water Resour. Res. 45 (W00A18). doi:10.1029/2008WR006963.

Seiler, K-P., Gat, J.R., 2007. Groundwater recharge from run-off, infiltration and percolation. Water Science and Technology Library, vol. 55. Springer.

Sheil, R.J., Costelloe, J.F., Reid, J.R.W., Hudson, P., 2006. Zooplankton diversity and assemblages in arid zone rivers of the Lake Eyre Basin, Australia. Marine Freshwater Res. 57, 49–60.

Sheldon, F., Boulton, A.J., Puckridge, J.T., 2002. Conservation value of variable connectivity: aquatic invertebrate assemblages of channel and floodplain habitats of a central Australian arid-zone river, Cooper Creek. Biol. Conserv. 103, 13–31.

Shibuo, Y., Jarsjo, J., Destouni, G., 2006. Bathymetry-topography effects on saltwater–fresh groundwater interactions around the shrinking Aral Sea. Water Resour. Res. 42, W11410.

Simmers, I., 1997. Groundwater recharge principles, problems and developments. Recharge of Phreatic Aquifers in (Semi-) arid Areas. Ed: I. Simmers. Balkema, Rotterdam (Chapter 1).

Simmers, I., 2003. Understanding Water in a Dry Environment; Hydrological Processes in Arid and Semi-arid Zonesm, vol. 23. IAH International Contributions to Hydrogeology, Balkema.

Subyani, A., Şen, Z., 2006. Refined chloride mass-balance method and its application in Saudi Arabia. Hydrol. Process. 20, 4373–4380.

Suess, H., 1971. Climatic changes and atmospheric radiocarbon. Palaeogeogr. Palaeoclimatol. Palaeoecol. 10, 199–202.

Tang, C., Chen, J., Shindo, S., Sakura, Y., Zhang, W., Shen, Y., 2004. Assessment of groundwater contamination by nitrates associated with wastewater irrigation: a case study in Shijiazhuang region, China. Hydrol. Process. 18, 2303–2312.

Thorburn, P.J., Walker, G.R., Woods, P.H., 1992. Comparison of diffuse discharge from shallow water tables in soils and salt flats. J. Hydrol. 136, 253–274.

Tweed, S.O., Leblanc, M., Webb, J.A., Lubczynski, M.W., 2007. Remote sensing and GIS for mapping groundwater recharge and discharge areas in salinity prone catchments, South-East Australia. Hydrogeol. J. 15, 75–96.

Ullman, W.J., 1985. Evaporation rate from a salt pan: estimates from chemical profiles in near-surface groundwaters. J. Hydrol. 79, 365–373.

Vermote, E.F., Vermeulen, A., 1999. Atmospheric Correction Algorithm: Spectral Reflectances (MOD09). Algorithm Theoretical Background Document. <http://modis.gsfc.nasa.gov/data/atbd/atbd_mod08.pdf>.

Vermote, E.F., El Saleous, N., Justice, C.O., Kaufman, Y.J., Privette, J.L., Remer, L., Roger, J.C., Tanré, D., 1997. Atmospheric correction of visible to middle-infrared EOS-MODIS data over land surfaces: background, operational algorithm and validation. J. Geophys. Res. 102 (D14), 17131–17141.

Weyhenmeyer, C.E., Burns, S.J., Waber, H.N., Macumber, P.G., Matter, A., 2002. Isotope study of moisture sources, recharge areas, and groundwater flow paths within the eastern Batinah coastal plain, Sultanate of Oman. Water Resour. Res. 38 (10), 1184. doi:10.1029/2000WR000149.

Williams, W.D., 2002. Environmental threats to salt lakes and the likely status of inland saline ecosystems in 2025. Environ. Conserv. 29 (2), 154–167.

Wolski, P., Savenije, H.H.G., 2006. Dynamics of floodplain-island groundwater flow in the Okavango Delta, Botswana. J. Hydrol. 320, 283–301.

Wood, W.W., Sanford, W.E., 2007. Atmospheric bromine flux from the coastal Abu Dhabi sabkhat: a ground-water mass-balance investigation. Geophys. Res. Lett. 34 (L14405). doi:10.1029/2007GL029922.

Wright, M.J., Fitzpatrick, R.W., Wells, C.B., 1990. Soils. In: Tyler, M.J., Twidale, C.R., Davies, M., Wells, C.B. (Eds.), Natural History of the North East Deserts. Royal Society of Australia Inc., pp. 61–74 (Chapter 4).

Yechieli, Y., Sivan, O., 2011. The distribution of saline groundwater and its relation to the hydraulic conditions of aquifers and aquitards: examples from Israel. Hydrogeol. J. 19, 71–81.

Zongyu, C., Zhenlong, N., Zhaoji, Z., Jixiang, Q., Yunju, N., 2005. Isotopes and sustainability of ground water resources, North China Plain. Ground water 43 (4), 485–493.